

GRL-0519, a Novel Oxatricyclic Ligand-Containing Nonpeptidic HIV-1 Protease Inhibitor (PI), Potently Suppresses Replication of a Wide Spectrum of Multi-PI-Resistant HIV-1 Variants *In Vitro*

Masayuki Amano,^a Yasushi Tojo,^a Pedro Miguel Salcedo-Gómez,^a Joseph Richard Campbell,^a Debananda Das,^d Manabu Aoki,^{a,b} Chun-Xiao Xu,^c Kalapala Venkateswara Rao,^c Arun K. Ghosh,^c Hiroaki Mitsuya^{a,d}

Departments of Infectious Diseases and Hematology, Kumamoto University School of Medicine, Kumamoto, Japan^a; Department of Medical Technology, Kumamoto Health Science University, Kumamoto, Japan^b; Departments of Chemistry and Medicinal Chemistry, Purdue University, West Lafayette, Indiana, USA^c; Experimental Retrovirology Section, HIV and AIDS Malignancy Branch, National Cancer Institute, National Institutes of Health, Bethesda, Maryland, USA^d

We report that GRL-0519, a novel nonpeptidic human immunodeficiency virus type 1 (HIV-1) protease inhibitor (PI) containing *tris*-tetrahydrofuranylurethane (*tris*-THF) and a sulfonamide isostere, is highly potent against laboratory HIV-1 strains and primary clinical isolates (50% effective concentration [EC₅₀], 0.0005 to 0.0007 μM) with minimal cytotoxicity (50% cytotoxic concentration [CC₅₀], 44.6 μM). GRL-0519 blocked the infectivity and replication of HIV-1_{NL4-3} variants selected by up to a 5 μM concentration of ritonavir, lopinavir, or atazanavir (EC₅₀, 0.0028 to 0.0033 μM). GRL-0519 was also potent against multi-PI-resistant clinical HIV-1 variants isolated from patients who no longer responded to existing antiviral regimens after long-term antiretroviral therapy, highly darunavir (DRV)-resistant variants, and HIV-2_{ROD}. The development of resistance against GRL-0519 was substantially delayed compared to other PIs, including amprenavir (APV) and DRV. The effects of nonspecific binding of human serum proteins on GRL-0519's antiviral activity were insignificant. Our analysis of the crystal structures of GRL-0519 (3OK9) and DRV (2IEN) with protease suggested that the *tris*-THF moiety, compared to the *bis*-THF moiety present in DRV, has greater water-mediated polar interactions with key active-site residues of protease and that the *tris*-THF moiety and parame-thoxy group effectively fill the S2 and S2' binding pockets, respectively, of the protease. The present data demonstrate that GRL-0519 has highly favorable features as a potential therapeutic agent for treating patients infected with wild-type and/or multi-PI-resistant variants and that the *tris*-THF moiety is critical for strong binding of GRL-0519 to the HIV protease substrate binding site and appears to be responsible for its favorable antiretroviral characteristics.

Combination antiretroviral therapy (cART) has had a major impact on the AIDS epidemic in industrially advanced nations. Recent analyses have revealed that mortality rates for human immunodeficiency virus type 1 (HIV-1)-infected persons have become close to those of the general population (1–4). However, eradication of HIV-1 does not appear to be currently possible, in part due to the viral reservoirs remaining in blood and infected tissues. Moreover, we have encountered a number of challenges in bringing the optimal benefits of the currently available therapeutics for AIDS and HIV-1 infection to individuals receiving cART (5–7). They include (i) drug-related toxicities, (ii) inability to fully restore normal immunologic functions once individuals developed AIDS, (iii) development of various cancers as a consequence of survival prolongation, (iv) flaring up of inflammation in individuals receiving cART or immune reconstruction syndrome (IRS), and (v) increased cost of antiviral therapy. Such limitations and flaws of cART are exacerbated by the development of drug-resistant HIV-1 variants (8–12), although the recent first-line cART with boosted protease inhibitor (PI)-based regimens has made the development of HIV-1 resistance less likely over an extended period of time (13).

Successful antiviral drugs, in theory, produce their virus-specific effects by interacting with viral receptors, virus-encoded enzymes, viral structural components, viral genes, or their transcripts without disturbing cellular metabolism or function. However, at present, no antiretroviral drugs or agents are likely to be completely specific for HIV-1 or to be devoid of toxicity or side effects in the therapy of AIDS. This is a critical issue, because

patients with AIDS and its related diseases will have to receive antiretroviral therapy for a long time, perhaps for the rest of their lives. Thus, the identification of new classes of antiretroviral drugs that have a unique mechanism(s) of action and produce no or minimal side effects remains an important therapeutic objective.

We have been focusing on the design and synthesis of nonpeptidyl PIs that are potent against HIV-1 variants resistant to the currently approved PIs. One such anti-HIV-1 agent, darunavir (DRV) (Fig. 1), containing a structure-based designed privileged nonpeptidic P2 ligand, 3(*R*),3a(*S*),6a(*R*)-*bis*-tetrahydrofuranylurethane (*bis*-THF) (14–16), has been approved as a first-line therapeutic agent for the treatment of individuals who are infected with HIV-1. In the present work, we examined and characterized the nonpeptidic HIV-1 protease inhibitors GRL-0519 (17) and its stereoisomer, GRL-0529, both of which contain the *tris*-THF moiety and a sulfonamide isostere. We found that GRL-0519 exerts highly potent activity against a wide spectrum of laboratory HIV-1

Received 8 November 2012 Returned for modification 3 December 2012

Accepted 5 February 2013

Published ahead of print 12 February 2013

Address correspondence to Hiroaki Mitsuya, hm21q@nih.gov.

Supplemental material for this article may be found at <http://dx.doi.org/10.1128/AAC.02189-12>.

Copyright © 2013, American Society for Microbiology. All Rights Reserved.

doi:10.1128/AAC.02189-12

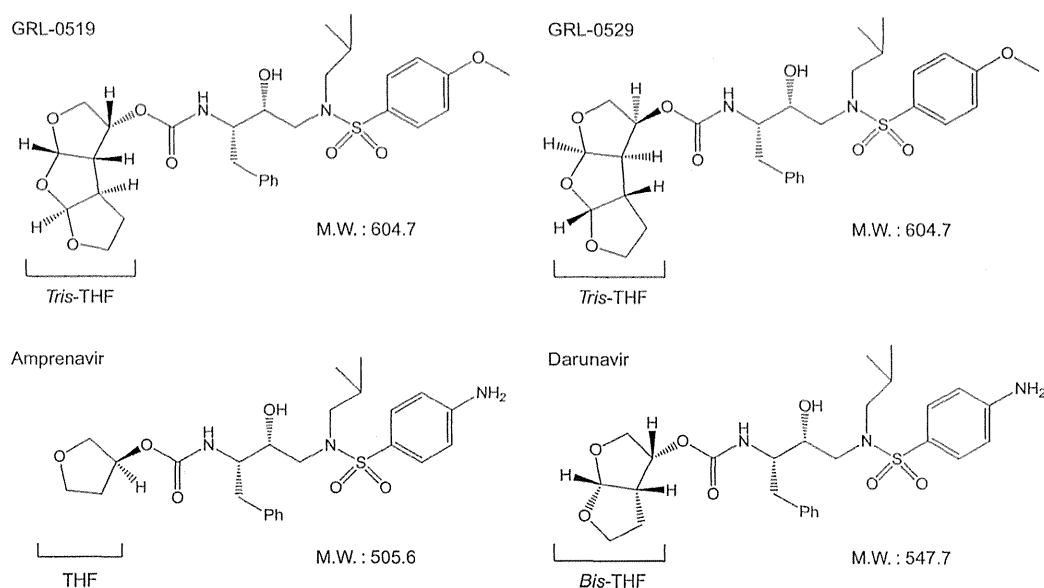


FIG 1 Structures of GRL-0519, GRL-0529, amprenavir, and darunavir. M.W., molecular weight.

strains and primary clinical isolates, including multi-PI-resistant variants with minimal cytotoxicity. In addition, GRL-0519 was active against HIV-2_{ROD}, as well as HIV-1 isolates examined. We also selected HIV-1 variants with GRL-0519 by propagating a laboratory wild-type HIV-1_{NL4-3} in MT-4 cells in the presence of increasing concentrations of GRL-0519 and determined the amino acid substitutions that emerged under the pressure of GRL-0519 in the protease-encoding region. In addition, we evaluated the effects of nonspecific binding of physiological human serum proteins on GRL-0519's anti-HIV-1 activity. We further analyzed the previously published crystal structure of GRL-0519 with protease (Protein Data Bank [PDB] ID, 3OK9) to gain a better understanding of the present antiviral data. The crystal structure analyses indicated that GRL-0519 has strong polar interactions with key residues in the active site of the protease. GRL-0519 also has several water-mediated polar interactions and tight van der Waals interactions with protease residues, suggesting that GRL-0519 binds very tightly in the active site of the protease.

MATERIALS AND METHODS

Cells and viruses. MT-2 and MT-4 cells were grown in RPMI 1640-based culture medium supplemented with 10% fetal calf serum (FCS) (JRH Biosciences, Lenexa, MD), 50 units/ml penicillin, and 100 μ g/ml kanamycin. The following HIV strains were employed for the drug susceptibility assay (see below): HIV-1_{LAI}, HIV-1_{NL4-3}, HIV-2_{ROD}, HIV-1_{ERS104prc} (18), clinical HIV-1 strains isolated from drug-naïve patients with AIDS, and six HIV-1 clinical strains that were originally isolated from patients with AIDS who had received 9 to 11 anti-HIV-1 drugs over the past 32 to 83 months and that were genotypically and phenotypically characterized as multi-PI-resistant HIV-1 variants (19, 20). All primary HIV-1 strains were passaged once or twice in 3-day-old phytohemagglutinin-activated peripheral blood mononuclear cells (PHA-PBM), and the virus-containing culture supernatants were stored at -80°C until they were used as sources of infectious virions.

Antiviral agents and human serum proteins. Roche Products Ltd. (Welwyn Garden City, United Kingdom) and Abbott Laboratories (Abbott Park, IL) kindly provided saquinavir (SQV) and ritonavir (RTV), respectively. Amprenavir (APV) was a courtesy gift from GlaxoSmith-

Kline, Research Triangle Park, NC. Lopinavir (LPV) was kindly provided by Japan Energy Inc., Tokyo, Japan. Atazanavir (ATV) was a contribution from Bristol Myers Squibb (New York, NY). Darunavir (DRV) was synthesized as previously described (21). Human serum albumin (HSA) and α 1-acid glycoprotein (AAG) were purchased from Sigma-Aldrich (St. Louis, MO).

Drug susceptibility assay. The susceptibility of HIV-1_{LAI} or HIV-2_{ROD} to various drugs was determined as previously described with minor modifications. Briefly, MT-2 cells (10^4 /ml) were exposed to 100 50% tissue culture infectious doses (TCID₅₀) of HIV-1_{LAI} or HIV-2_{ROD} in the presence or absence of various concentrations of drugs in 96-well microculture plates and incubated at 37°C for 7 days. After incubation, 100 μ l of the medium was removed from each well and 3-(4,5-dimethylthiazol-2-yl)-2,5-diphenyltetrazolium bromide (MTT) solution (10 μ l, 7.5 mg/ml in phosphate-buffered saline) was added to each well in the plate, followed by incubation at 37°C for 2 h. After incubation to dissolve the formazan crystals, 100 μ l of acidified isopropanol containing 4% (vol/vol) Triton X-100 was added to each well, and the optical density was measured in a kinetic microplate reader (Vmax; Molecular Devices, Sunnyvale, CA). All assays were performed in duplicate or triplicate. In some experiments, MT-2 cells were chosen as target cells in the MTT assay, since these cells undergo greater HIV-1-elicited cytopathic effects than MT-4 cells. To determine the sensitivity of primary HIV-1 isolates to drugs, PHA-PBM (10^6 /ml) were exposed to 50 TCID₅₀ of each primary HIV-1 isolate and cultured in the presence or absence of various concentrations of drugs in 10-fold serial dilutions in 96-well microculture plates. In determining the drug susceptibilities of certain laboratory HIV-1 strains, MT-4 cells were employed as target cells as previously described, with minor modifications. In brief, MT-4 cells (10^5 /ml) were exposed to 100 TCID₅₀ of drug-resistant HIV-1 strains in the presence or absence of various concentrations of drugs and incubated at 37°C . On day 7 of culture, the supernatants were harvested and the amounts of p24 (capsid [CA]) Gag protein were determined by using a fully automated chemiluminescent enzyme immunoassay system (Lumipulse F; Fujirebio Inc., Tokyo, Japan) (22, 23). Drug concentrations that suppressed the production of p24 Gag protein by 50% (50% effective concentration [EC₅₀]) were determined by comparison with the p24 production level in a drug-free control cell culture. All assays were performed in duplicate or triplicate. PHA-PBM were derived from a single donor in each independent experiment. Thus, to obtain the data,

three different healthy donors were recruited. For determining the anti-retroviral activity and cytotoxicity of a drug, we used the same cells and cultured them for the same 7 days. The MTT assay was employed for HIV-1_{LAI} and HIV-2_{ROD}, while the p24 assay was employed for clinical HIV-1 isolates and drug-resistant HIV-1 strains.

Creation of PI-resistant HIV-1 variants *in vitro*. MT-4 cells (10⁵/ml) were exposed to HIV-1_{NL4-3} (500 TCID₅₀) and cultured in the presence of various PIs at an initial concentration equal to its EC₅₀. Viral replication was monitored by the determination of the amount of p24 Gag produced by MT-4 cells. The culture supernatants were harvested on day 7 and were used to infect fresh MT-4 cells for the next round of culture in the presence of increasing concentrations of each drug. When the virus began to propagate in the presence of the drug, the drug concentration was increased generally 2- to 3-fold. Proviral DNA samples obtained from the lysates of infected cells were subjected to nucleotide sequencing. This drug selection procedure was carried out until the drug concentration reached 5 μM, as previously described (24–26). In the experiments for selecting drug-resistant variants, MT-4 cells were also exploited as target cells, since HIV-1 in general replicates at higher levels in MT-4 cells than in MT-2 cells, as described above.

Determination of nucleotide sequences. Molecular cloning and determination of the nucleotide sequences of HIV-1 strains passaged in the presence of anti-HIV-1 agents were performed as previously described (24). In brief, high-molecular-weight DNA was extracted from HIV-1-infected MT-4 cells by using the InstaGene Matrix (Bio-Rad Laboratories, Hercules, CA) and was subjected to molecular cloning, followed by sequence determination. The primers used for the first round of PCR with the entire Gag- and protease-encoding regions of the HIV-1 genome were LTR F1 (5'-GAT GCT ACA TAT AAG CAG CTG C-3') and PR12 (5'-CTC GTG ACA AAT TTC TAC TAA TGC-3'). The first-round PCR mixture consisted of 1 μl of proviral DNA solution, 10 μl of Premix Taq (Ex Taq version; TaKaRa Bio Inc., Otsu, Japan), and 10 pmol of each of the first PCR primers in a total volume of 20 μl. The PCR conditions used were an initial 3 min at 95°C, followed by 35 cycles of 40 s at 95°C, 20 s at 55°C, and 2 min at 72°C, with a final 10 min of extension at 72°C. The first-round PCR products (1 μl) were used directly in the second round of PCR with primers LTR F2 (5'-GAG ACT CTG GTA ACT AGA GAT C-3') and KSMA2.1 (5'-CCA TCC CGG GCT TTA ATT TTA CTG GTA C-3') under the following PCR conditions: an initial 3 min at 95°C, followed by 35 cycles of 30 s at 95°C, 20 s at 55°C, and 2 min at 72°C, with a final 10 min of extension at 72°C (a stick diagram of HIV-1 genome PCR amplification for sequence analysis is shown in Fig. S1 in the supplemental material). The second-round PCR products were purified with spin columns (MicroSpin S-400 HR columns; Amersham Biosciences Corp., Piscataway, NJ), cloned directly, and subjected to sequencing with a model 3130 automated DNA sequencer (Applied Biosystems, Foster City, CA).

Determination of replication kinetics of GRL-0519-resistant HIV-1_{NL4-3} variants and wild-type HIV-1_{NL4-3}. The GRL-0519-resistant variant at passage 37 was propagated in fresh MT-4 cells without GRL-0519 for 7 days, and aliquoted HIV-1_{519^RP37} viral stocks were stored at -80°C until use. MT-4 cells (3.2 × 10⁵) were exposed to the HIV-1_{519^RP37} or wild-type HIV-1_{NL4-3} preparation containing 10 ng/ml p24 in 6-well culture plates for 3 h, and the newly infected MT-4 cells were washed with fresh medium and divided into 4 fractions, each cultured with or without GRL-0519 (final concentration of MT-4 cells, 10⁴/ml; drug concentrations, 0, 0.005, 0.01, and 0.015 μM). The amounts of p24 were measured every 2 days for up to 7 days.

Generation of recombinant HIV-1 clones. To generate HIV-1 clones carrying the desired amino acid substitutions, site-directed mutagenesis was performed with a QuikChange site-directed mutagenesis kit (Stratagene, La Jolla, CA), and the amino acid substitution-containing genomic fragments were introduced into pHIV-1_{NL4-3SmaI}. Determination of the nucleotide sequences of the plasmids confirmed that each clone had the desired amino acid substitution but no unintended amino acid substitutions. Each recombinant plasmid was transfected into COS7 cells with

TABLE 1 Antiviral activities of GRL-0519 and -0529 against HIV-1_{LAI} or HIV-2_{ROD}

Compound	EC ₅₀ (μM) ^a		CC ₅₀ (μM) (±SD)	Selectivity index ^b
	HIV-1 _{LAI}	HIV-2 _{ROD}		
GRL-0519	0.0007 ± 0.0005	0.0004 ± 0.0002	44.6 ± 3.5	63,714
GRL-0529	0.33 ± 0.04	0.40 ± 0.06	38.7 ± 3.7	118
SQV	0.026 ± 0.006	0.003 ± 0.001	19.8 ± 2.9	773
APV	0.033 ± 0.002	0.37 ± 0.11	84.7 ± 5.4	2,590
ATV	0.0048 ± 0.0001	0.0077 ± 0.0006	27.6 ± 2.7	5,520
DRV	0.0042 ± 0.0006	0.0088 ± 0.0004	152.7 ± 10.1	36,357

^a MT-2 cells (10⁴/ml) were exposed to 100 TCID₅₀ of HIV-1_{LAI} or HIV-2_{ROD} and cultured in the presence of various concentrations of each PI, and the EC₅₀ values were determined using the MTT assay. All assays were conducted in duplicate, and the data shown represent mean value (±1 standard deviation [SD]) derived from the results of three independent experiments.

^b Each selectivity index denotes a ratio of CC₅₀ to EC₅₀ against HIV-1_{LAI}.

Lipofectamine LTX transfection reagent (Invitrogen, Carlsbad, CA), and the infectious virions thus made were harvested for 72 h after transfection and stored at -80°C until use.

Structural analysis of interactions of GRL-0519 and DRV with protease. The crystal structures of HIV-1 protease complexed with GRL-0519 or DRV were obtained from the protein data bank (PDB ID, 3OK9 and 2IEN, respectively). The inhibitor conformation with the higher occupancy in the crystal structure was considered for analysis. Bond orders were properly assigned to the inhibitor molecules. Hydrogens were added to all the heavy atoms, and their positions were optimized in an OPLS2005 force field (27) with constraints on heavy atom positions. A cutoff distance of 3.0 Å between a polar hydrogen and oxygen or nitrogen was used to determine the presence of hydrogen bonds. The structures were analyzed using Maestro version 9.3 (Schrödinger, LLC, New York, NY, 2012).

RESULTS

Antiviral activities of GRL-0519 and -0529 against HIV-1_{LAI} and HIV-2_{ROD} and their cytotoxicities. We first examined the antiviral potencies of GRL-0519 and -0529 against a variety of HIV-1 isolates. GRL-0529 showed only moderate anti-HIV-1 activity against a laboratory wild-type HIV-1 strain, HIV-1_{LAI}, and an HIV-2 strain, HIV-2_{ROD}, with EC₅₀s of 0.33 and 0.40 μM, respectively (Table 1). Conversely, GRL-0519 was extremely potent against HIV-1_{LAI}, with an EC₅₀ of 0.0007 μM compared to other clinically available Food and Drug Administration (FDA)-approved PIs examined, including DRV (Table 1), as assessed with the MTT assay using MT-2 target cells, while its cytotoxicity was evident only at high concentrations (50% cytotoxic concentration [CC₅₀], 44.6 μM) and the selectivity index proved to be highly favorable at 63,714 (Table 1). GRL-0519 was also very potent against HIV-2_{ROD}, with an EC₅₀ of 0.0004 μM (Table 1).

GRL-0519 is potent against various PI-selected laboratory HIV-1 variants. We also examined GRL-0519 against an array of HIV-1_{NL4-3} variants, which had been selected by propagating HIV-1_{NL4-3} in the presence of increasing concentrations (up to 5 μM) of each of 4 FDA-approved PIs (RTV, APV, ATV, and LPV) in MT-4 cells (24). Such variants had acquired various PI resistance-associated amino acid substitutions in the protease-encoding region of the viral genome (Table 2, note a). Each variant was highly resistant to the PI by which the variant was selected and showed significant resistance, with an EC₅₀ of >1 μM. GRL-0519 was highly active against all the variants (except HIV-1_{APV^R5μM}), with EC₅₀s of 2.8 to 3.3 nM (differences were 6- to 7-fold greater compared to those against HIV-1_{NL4-3}) (Table 2).

TABLE 2 Antiviral activities of GRL-0519 and -0529 against laboratory PI-resistant HIV-1 variants

Virus ^a	EC ₅₀ (nM) ^b						
	GRL-0519	GRL-0529	APV	ATV	LPV	TPV	DRV
HIV-1 _{NL4-3}	0.5 ± 0.1	356.3 ± 33.8	24.9 ± 0.1	4.2 ± 1.1	37.8 ± 4.5	362.9 ± 104.4	3.9 ± 0.6
HIV-1 _{RTV^R_{5μM}}	2.8 ± 0.4 (6)	504.3 ± 26.6 (1)	532.9 ± 25.9 (21)	36.4 ± 3.0 (9)	501.2 ± 44.9 (13)	402.1 ± 56.1 (1)	29.1 ± 2.1 (7)
HIV-1 _{APV^R_{5μM}}	38.0 ± 0.9 (76)	>1,000 (>3)	>1,000 (>40)	371.0 ± 7.8 (88)	>1,000 (>26)	>1,000 (>3)	368.5 ± 32.4 (94)
HIV-1 _{ATV^R_{5μM}}	3.3 ± 1.6 (7)	376.9 ± 164.8 (1)	390.0 ± 11.1 (16)	>1,000 (>238)	>1,000 (>26)	>1,000 (>3)	28.1 ± 6.4 (7)
HIV-1 _{LPV^R_{5μM}}	3.2 ± 0.4 (7)	>1,000 (>3)	420.1 ± 61.9 (17)	35.1 ± 4.7 (8)	>1,000 (>26)	>1,000 (>3)	32.9 ± 1.3 (8)

^a The amino acid substitutions identified in the protease-encoding region compared to the wild-type HIV-1_{NL4-3} include the following: M46I, V82F, and I84V in HIV-1_{RTV^R_{5μM}}; L10F, V32I, M46I, I54 M, A71V, and I84V in HIV-1_{APV^R_{5μM}}; L23I, E34Q, K43I, M46I, I50L, G51A, L63P, A71V, V82A, and T91A in HIV-1_{ATV^R_{5μM}}; and L10F, M46I, I54V, and V82A in HIV-1_{LPV^R_{5μM}}.

^b The EC₅₀ values were determined by using MT-4 cells as target cells. MT-4 cells (10⁵/ml) were exposed to 100 TCID₅₀ of each HIV-1 strain, and the inhibition of p24 Gag protein production by each drug was used as an endpoint. The numbers in parentheses represent the fold changes of EC₅₀s for each isolate compared to the EC₅₀s for HIV-1_{NL4-3}. All assays were conducted in duplicate or triplicate, and the data shown represent mean values (±1 SD) derived from the results of two or three independent experiments.

GRL-0519 exerts potent activity against highly PI-resistant clinical HIV-1 isolates. In our previous work, we isolated highly multi-PI-resistant primary HIV-1 strains, HIV-1_{MDR/B}, HIV-1_{MDR/C}, HIV-1_{MDR/G}, HIV-1_{MDR/TM}, HIV-1_{MDR/MM}, and HIV-1_{MDR/JSL}, from patients with AIDS who had failed then-existing anti-HIV regimens after receiving 9 to 11 anti-HIV-1 drugs over 32 to 83 months (19, 20). These primary strains contained 9 to 14 amino acid substitutions in the protease-encoding region, which have reportedly been associated with HIV-1 resistance against various PIs (Table 3, note a). The potency of APV, ATV, and LPV against such clinical multidrug-resistant HIV-1 strains was significantly compromised, as examined in PHA-PBM as target cells using p24 production inhibition as an endpoint (Table 3). However, GRL-0519 exerted quite potent antiviral activity, and its EC₅₀s against those clinical variants were quite low: 0.8 to 3.4 nM (Table 3). The antiviral activity of GRL-0519 proved to be most

potent against the six multidrug-resistant clinical HIV-1 variants examined compared to the four FDA-approved PIs (APV, ATV, LPV, and DRV). We also examined the antiviral activity of GRL-0519 against highly DRV-resistant variants (28). These variants were created using the mixture of 8 highly multi-PI-resistant clinical isolates as a starting HIV-1 source and selected with increasing concentrations of DRV. GRL-0519 maintained its activity against highly DRV-resistant MDR mixtures (EC₅₀, 5.6 to 30.0 nM), being more potent than DRV by 7.8- to 8.5-fold (Table 3). Overall, GRL-0519 exerted stronger antiviral activity against various wild-type HIV-1 strains, drug-resistant variants, and HIV-2 strains than DRV by 5- to 22-fold. Furthermore, GRL-0519 was more potent than APV by 118- to 925-fold against HIV-2_{ROD} and drug-resistant variants (Tables 1 to 3).

Effects of human serum proteins on the antiretroviral activity of GRL-0519. The binding of human serum proteins to a

TABLE 3 Antiviral activities of GRL-0519 and -0529 against multidrug-resistant clinical isolates and highly DRV-resistant MDR mixtures in PHA-PBM

Virus ^a	EC ₅₀ (nM) ^b					
	GRL-0519	GRL-0529	APV	ATV	LPV	DRV
HIV-1 _{WT/ERS104pre}	0.6 ± 0.2	347.4 ± 27.3	33.8 ± 5.1	2.7 ± 0.6	31.4 ± 4.2	3.9 ± 0.6
HIV-1 _{MDR/B} (X4)	3.4 ± 0.5 (6)	611.8 ± 72.8 (2)	459.4 ± 99.2 (14)	469.7 ± 7.4 (174)	> 1,000 (>32)	27.8 ± 5.9 (7)
HIV-1 _{MDR/C} (X4)	0.8 ± 0.2 (1)	514.4 ± 130.6 (1)	346.1 ± 55.2 (10)	38.8 ± 2.8 (14)	436.5 ± 3.5 (14)	10.3 ± 2.4 (3)
HIV-1 _{MDR/G} (X4)	2.6 ± 1.3 (4)	655.8 ± 292.9 (2)	462.6 ± 64.5 (14)	19.4 ± 7.5 (7)	181.3 ± 23.0 (6)	27.8 ± 5.2 (7)
HIV-1 _{MDR/TM} (X4)	2.1 ± 0.3 (4)	530.0 ± 74.7 (2)	476.4 ± 8.1 (14)	74.5 ± 2.6 (28)	422.9 ± 82.0 (13)	30.0 ± 1.0 (8)
HIV-1 _{MDR/MM} (R5)	2.5 ± 0.5 (4)	787.4 ± 251.4 (2)	338.9 ± 15.5 (10)	204.8 ± 23.5 (76)	622.5 ± 82.0 (20)	13.3 ± 6.2 (3)
HIV-1 _{MDR/JSL} (R5)	2.5 ± 0.2 (4)	> 1,000 (>3)	436.3 ± 90.4 (13)	211.3 ± 98.6 (78)	> 1,000 (>32)	22.1 ± 9.3 (6)
HIV-1 _{DRV^R_{10P}}	5.6 ± 0.4 (9)	> 1,000 (>3)	> 1,000 (>32)	322.9 ± 10.4 (77)	> 1,000 (>32)	43.4 ± 13.4 (11)
HIV-1 _{DRV^R_{20P}}	30.0 ± 9.8 (50)	> 1,000 (>3)	> 1,000 (>32)	> 1,000 (>370)	> 1,000 (>32)	255.2 ± 4.0 (64)

^a The amino acid substitutions identified in the protease-encoding region compared to the consensus type B sequence cited from the Los Alamos database include the following: L63P in HIV-1_{ERS104pre}; L10I, K14R, L33I, M36I, M46I, F53I, K55R, I62V, L63P, A71V, G73S, V82A, L90 M, and I93L in HIV-1_{MDR/B}; L10I, I15V, K20R, L24I, M36I, M46L, I54V, I62V, L63P, K70Q, V82A, and L89 M in HIV-1_{MDR/C}; L10I, V11I, T12E, I15V, L19I, R41K, M46L, L63P, A71T, V82A, and L90 M in HIV-1_{MDR/G}; L10I, K14R, R41K, M46L, I54V, L63P, A71V, V82A, L90 M, and I93L in HIV-1_{MDR/TM}; L10I, K43T, M46L, I54V, L63P, A71V, V82A, L90 M, and Q92K in HIV-1_{MDR/MM}; L10I, L24I, I33F, E35D, M36I, N37S, M46L, I54V, R57K, I62V, L63P, A71V, G73S, and V82A in HIV-1_{MDR/JSL}; L10I, I15V, K20R, L24I, V32I, M36I, M46L, I54V, I62V, L63P, K70Q, V82A, and L88 M in HIV-1_{DRV^R_{10P}}; and L10I, I15V, K20R, L24I, V32I, M36I, M46L, L63P, A71T, V82A, and L88 M in HIV-1_{DRV^R_{20P}}. HIV-1_{ERS104pre} served as a source of wild-type HIV-1. DRV-resistant HIV-1 variants (HIV-1_{DRV^R_{10P}} and HIV-1_{DRV^R_{20P}}) were selected *in vitro* by propagating a mixture of eight HIV-1_{MDR} isolates in the presence of increasing concentrations of DRV in MT-4 cells. Six of the eight isolates were the same as those described above. Amino acid substitutions identified in proteases of the other two isolates compared to the consensus type B sequence cited from the Los Alamos database include the following: L10I, I15V, E35D, N37E, K45R, I54V, L63P, A71V, V82T, L90 M, I93L, and C95F in HIV-1_{MDR/A}; L10R, N37D, M46I, I62V, L63P, A71V, G73S, V74I, V82T, L90 M, and I93L in HIV-1_{MDR/SS}.

^b The EC₅₀ values were determined by using PHA-PBM as target cells, and the inhibition of p24 Gag protein production by each drug was used as an endpoint. The numbers in parentheses represent the fold changes of EC₅₀s for each isolate compared to the EC₅₀s for HIV-1_{ERS104pre}. All assays were conducted in duplicate or triplicate, and the data shown represent mean values (±1 SD) derived from the results of three independent experiments. PHA-PBM were derived from a single donor in each independent experiment.

TABLE 4 Nonspecific binding effects of human serum proteins on GRL-0519's antiviral activity

Compound	EC ₅₀ (nM) ^a		
	None	HSA	AAG
GRL-0519	0.6 ± 0.2	1.9 ± 1.1 (3)	2.4 ± 0.3 (4)
GRL-0529	347.4 ± 27.3	351.5 ± 22.7 (2)	649.0 ± 48.9 (2)
APV	31.5 ± 5.5	30.5 ± 2.6 (1)	286.3 ± 14.8 (9)
ATV	2.7 ± 0.6	14.6 ± 1.2 (5)	32.7 ± 15.9 (12)
LPV	31.4 ± 4.2	32.5 ± 2.7 (1)	232.1 ± 15.2 (7)
DRV	3.9 ± 1.0	7.4 ± 1.2 (2)	33.8 ± 3.5 (9)

^a HSA (40 mg/ml) or AAG (10 μM) was used to evaluate the binding effects of human serum proteins on GRL-0519 and -0529 antiviral activities. The EC₅₀ values against HIV-1_{ERS104pre} with or without HSA or AAG were determined by p24 assay using PHA-PBM as target cells, and the inhibition of p24 Gag production by each drug was used as an endpoint. The numbers in parentheses represent the fold changes of the EC₅₀ values compared to the values without HSA or AAG. The data shown represent mean values derived from the results of two or three independent experiments. PBM were derived from a single donor in each independent experiment.

drug is an important determinant of its pharmacological activity *in vivo*, because overly tight binding may result in reducing interactions between the drug and its target (29). We thus determined the effects of the binding of HSA and AAG on GRL-0519's antiretroviral activity *in vitro*. Physiologically normal concentrations of HSA (40 mg/ml) and AAG (10 μM) were used to evaluate their binding effects on GRL-0519's activity against a wild-type clinical isolate, HIV-1_{ERS104pre}. All four FDA-approved drugs substantially maintained their activity in the presence of HSA, with reduction of activity by up to 5-fold relative to the activity in the absence of additional HSA (Table 4). The activities of those PIs were reduced in the presence of AAG by 7- to 12-fold (Table 4). However, the binding effects of both HSA and AAG on GRL-0519's activity were insignificant, only a 3- to 4-fold difference. Of note, GRL-0519's EC₅₀s with HSA or AAG (1.9 to 2.4 nM) significantly exceeded those of the four FDA-approved PIs (Table 4).

In vitro selection of HIV-1 variants resistant to GRL-0519.

We next attempted to select HIV-1 variants resistant to GRL-0519 by propagating a laboratory HIV-1 strain, HIV-1_{NL4-3}, in MT-4 cells in the presence of increasing concentrations of GRL-0519 as previously described (24). HIV-1_{NL4-3} was initially exposed to 0.0007 μM GRL-0519 and underwent 37 passages, after which the concentration of GRL-0519 was found to have increased 19-fold (0.0131 μM) compared to that at the initiation of selection. Judging from the amounts of p24 Gag protein produced in the culture medium (up to ~282 ng/ml), the replicative capacity of HIV-1_{NL4-3} at passage 37 (HIV_{519^RP37}) was thought to have been reasonably well maintained. Compared to the kinetics of the emergence of variants resistant to APV, the emergence of GRL-0519- and DRV-resistant variants was substantially delayed (Fig. 2). Of note, HIV-1 variants resistant to APV and capable of replicating at >5 μM emerged by passage 20, and variants resistant to GRL-0529, replicating at >1 μM, emerged by passage 6, while it became fairly difficult to increase the concentrations of DRV and GRL-0519 around and beyond passage 20, since the virus populations ceased to replicate with further increased concentrations.

The protease-encoding region of the proviral DNA isolated from infected MT-4 cells was cloned and sequenced at passages 6, 13, 22, 29, and 37 under GRL-0519 selection. The sequences of the region cloned and the percent frequency of identical sequences at each passage are depicted in Fig. 3. By passage 13, the wild-type protease gene sequence was seen in 7 of 19 clones, although an N37S substitution was noted in 10 of the 19 clones. However, by passage 22 and beyond, N37S disappeared, and the virus had mostly acquired K43I and A71T substitutions. As the passages proceeded, greater numbers of amino acid substitutions emerged. At passage 29, V82I substitution was seen in 16 of 22 clones, and V82I became dominant by passage 37 (25 of 26 clones). An L33V substitution was also observed in 4 of the 26 clones by passage 37. Reportedly, APV-resistant HIV-1 variants contain V32I, I50V, I54L/M, L76V, I84V, and L90M substitutions (30, 31), and such substitutions were also identified in the present study (data not

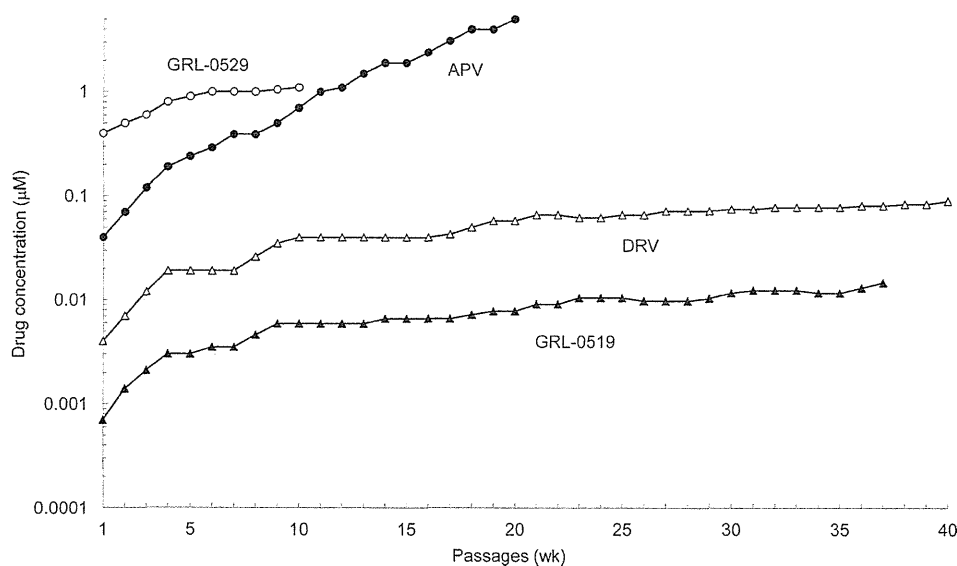


FIG 2 *In vitro* selection of PI-resistant HIV-1 variants. HIV-1_{NL4-3} was propagated in MT-4 cells in the presence of increasing concentrations of amprenavir (●), darunavir (△), GRL-0519 (▲), or GRL-0529 (○). Each passage of virus was conducted in a cell-free manner.

	10	20	30	40	50	60	70	80	90	99		
pNL4-3 PR	PQITLWQRPL	VTIKIGGOLK	EALLDTGADD	TVLEEMNLPG	RWKPKMIGGI	GGFIKVRQYD	QILIEICGKH	AIGTVLVGPT	PVNIIGRNLL	TQIGCTLNF		
6P-1		12/16
6P-2S.....		1/16
6P-3S.....		1/16
6P-4R.....		1/16
6P-5V.....A.....		1/16
13P-1S.....		8/19
13P-2		7/19
13P-3P.....		1/19
13P-4P.....S.....		1/19
13P-5S.....L.....		1/19
13P-6G.....		1/19
22P-1I.....T.....		10/14
22P-2I.....M.....T.....		1/14
22P-3S.....I.....T.....		1/14
22P-4V.....T.....		1/14
22P-5I.....T.....A.....		1/14
29P-1I.....T.....I.....		11/22
29P-2I.....T.....I.....		3/22
29P-3T.....I.....T.....L.....		1/22
29P-4I.....T.....I.....C.....		1/22
29P-5I.....T.....I.....A.....		1/22
29P-6I.....I.....T.....I.....		1/22
29P-7I.....T.....I.....T.....		1/22
29P-8M.....I.....I.....T.....I.....		1/22
29P-9G.....I.....I.....T.....I.....S.....		1/22
29P-10I.....I.....T.....T.....		1/22
37P-1I.....T.....I.....		17/26
37P-2V.....I.....T.....I.....		3/26
37P-3I.....V.....T.....I.....		1/26
37P-4I.....T.....I.....N.....		1/26
37P-5I.....V.....C.....T.....L.....		1/26
37P-6I.....T.....I.....A.....		1/26
37P-7A.....I.....I.....T.....I.....A.....Y.....		1/26
37P-8V.....I.....T.....I.....		1/26

FIG 3 Amino acid sequences of the protease-encoding regions of HIV-1_{NL4-3} variants selected in the presence of GRL-0519. The amino acid sequences of protease, deduced from the nucleotide sequence of the protease-encoding region of each proviral DNA isolated at each indicated time, are shown. The amino acid sequence of the wild-type HIV-1_{NL4-3} protease is illustrated at the top as a reference.

shown). However, no such APV resistance-associated amino acid substitutions emerged during the GRL-0519 selection (Fig. 3). Additionally, HIV-1 selected with GRL-0519 (HIV₅₁₉^R_{P37}) acquired the following Gag amino acid substitutions: E17K and V84A in the matrix (MA) region and G61E and D152N in the CA region.

HIV₅₁₉^R_{P37} fails to replicate at a low concentration of GRL-0519. Since the replicative capacity of HIV₅₁₉^R_{P37} was thought to

be reasonably well maintained despite the presence of GRL-0519, as mentioned above, we determined the replication kinetics of HIV₅₁₉^R_{P37} and HIV-1_{NL4-3}. As shown in Fig. 4A, HIV-1_{NL4-3} failed to replicate in the presence of as little as 0.005 μM GRL-0519 during the entire culture period of 7 days. However, HIV₅₁₉^R_{P37} was capable of replicating in the presence of 0.005 and 0.01 μM GRL-0519, and the amount of p24 produced in the culture

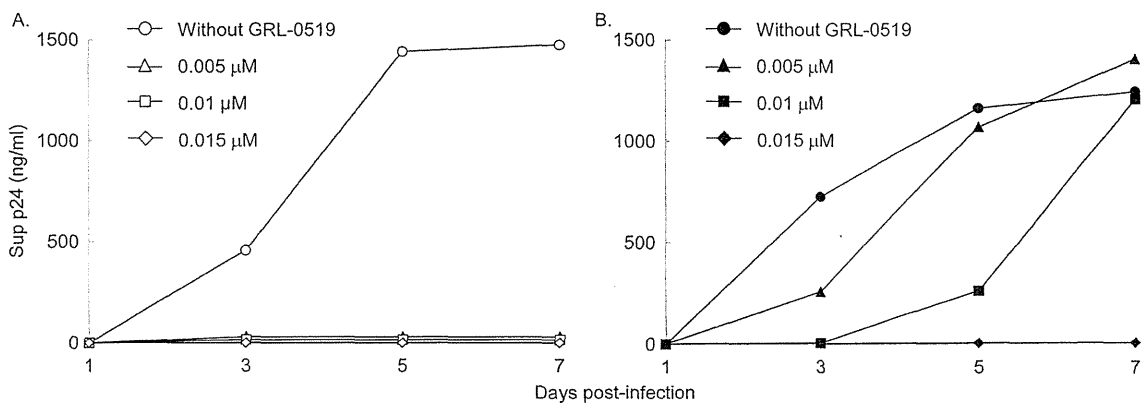


FIG 4 Replication kinetics of HIV-1_{NL4-3} and HIV₅₁₉^R_{P37}. MT-4 cells (3.2×10^5) were exposed to a HIV-1_{NL4-3} or HIV-1₅₁₉^R_{P37} preparation containing 10 ng/ml p24 in 6-well culture plates for 3 h, and the MT-4 cells were washed with fresh medium and divided into 4 fractions, each cultured with or without GRL-0519 (final concentration of MT-4 cells, 10^4 /ml; drug concentrations, 0, 0.005, 0.01, and 0.015 μM). The amount of p24 in each culture flask was measured every 2 days to 7 days, once at each time point.

TABLE 5 Roles of 3 amino acid substitutions that emerged during selection with GRL-0519 on GRL-0519's anti-HIV-1 activity

Virus ^a	GRL-0519 EC ₅₀ (nM) ^b
HIV-1 _{NL4-3}	0.5 ± 0.1
HIV-1 _{519^RP37}	6.0 ± 1.4 (12)
HIV-1 _{K43I}	1.2 ± 0.2 (2)
HIV-1 _{A71T}	1.4 ± 0.6 (3)
HIV-1 _{V82I}	3.2 ± 0.1 (6)

^a HIV-1_{K43I}, HIV-1_{A71T}, and HIV-1_{V82I} were created using a HIV-1_{NL4-3} plasmid clone.

^b The EC₅₀ values were determined with MT-4 cells, employing a p24 assay. The data shown represent mean values (±1 SD) derived from the results of two or four independent experiments. The numbers in parentheses represent the fold changes of EC₅₀s compared to the value against HIV-1_{NL4-3}.

medium reached the amount without GRL-0519 by day 7. However, HIV_{519^RP37} failed to replicate in the presence of 0.015 μM GRL-0519, and no p24 was detected throughout the culture period (Fig. 4B).

Roles of 3 amino acid substitutions that emerged during selection with GRL-0519 in GRL-0519's anti-HIV-1 activity. We also examined the roles of 3 substitutions that emerged during the GRL-0519 selection experiment, K43I, A71T, and V82I, using single-amino-acid substitutions carrying HIV-1_{NL4-3} variants. First, we determined the exact EC₅₀ of GRL-0519 against HIV_{519^RP37} using a p24 assay. GRL-0519 suppressed the replication of HIV_{519^RP37} with an EC₅₀ of 6.0 nM, 12-fold different from the EC₅₀ against HIV-1_{NL4-3} (Table 5). Next, we determined EC₅₀s of GRL-0519 against 3 single-amino-acid substitution-containing HIV-1_{NL4-3} variants (HIV-1_{K43I}, HIV-1_{A71T}, and HIV-1_{V82I}). GRL-0519 inhibited the replication of HIV-1_{K43I}, HIV-1_{A71T}, and HIV-1_{V82I} with EC₅₀s of 1.2, 1.4, and 3.2 nM, respectively (differences were 2-, 3-, and 6-fold compared to those against HIV-1_{NL4-3}, respectively) (Table 5).

In vitro selection of a mixture of 8 HIV-1_{MDR} variants resistant to GRL-0519. As described above and as shown in Fig. 2, the emergence of HIV-1 variants resistant to GRL-0519 was much delayed, and it took as many as 37 passages (37 weeks) for the virus to acquire its replicative activity in the presence of low concentrations (~0.01 μM). Thus, we attempted to select out GRL-0519-resistant variants using a mixture of 8 multidrug-resistant clinical isolates (HIV-1_{MDR}) as a starting HIV-1 population, as previously described (28, 32). We performed an additional selection experiment with MT4 cells and a mixture of 8 HIV-1_{MDR} variants as a starting virus population, with APV, DRV, and GRL-0519 and -0529. Similar to the results of selection experiments using MT-4 cells and HIV-1_{NL4-3}, the emergence of HIV-1 strains capable of replicating in the presence of GRL-0519 was significantly delayed compared to the cases with APV and DRV (Fig. 5).

Structural analyses of GRL-0519 interactions with protease.

We have recently reported the crystal structure depicting the binding mode and interactions of GRL-0519 with protease (17). GRL-0519 has a *tris*-THF moiety as its P2 ligand, and DRV has a *bis*-THF group as its P2 ligand (Fig. 1). Another difference is that GRL-0519 has a methoxybenzene as a P2' ligand, whereas DRV has an aniline. We analyzed the crystal structure of GRL-0519 with protease and compared it with the structure of protease complexed with DRV. We found that the oxygens of the first and second THF rings of GRL-0519 form hydrogen bond interactions with the backbone amide nitrogens of Asp-29 and Asp-30 in the S2

binding pocket of the protease (Fig. 6A). The urethane NH of GRL-0519 forms a hydrogen bond with Gly-27. The hydroxyl group of GRL-0519 forms hydrogen bonds with the catalytic Asp-25 and Asp-25'. The carbonyl oxygen and the sulfonamide oxygen of GRL-0519 form polar interactions with Ile-50 and Ile-50' in the protease flap through a bridging water molecule. These interactions are also seen for DRV (Fig. 6B). In fact, the polar interactions with Gly-27, Ile-50, and Ile-50', as well as with Asp-25 and Asp-25', are also seen for other protease inhibitors (33, 34). The oxygen of the methoxybenzene (P2' ligand) of GRL-0519 forms a hydrogen bond with the backbone amide nitrogen of Asp-30' in the S2' site of protease. This interaction at the S2' site is different in the case of DRV. DRV has an aniline as the P2' ligand, and it forms polar interactions with the backbone carbonyl oxygen of Asp-30'. The third THF ring of the *tris*-THF has water-mediated interactions with Thr-26 and Arg-8 involving 6 bridging water molecules. We also analyzed the van der Waals interactions between GRL-0519 and protease (Fig. 7). The methoxy moiety of GRL-0519 makes good van der Waals contacts with the Asp-29' and Asp-30' residues at the S2' site of protease (Fig. 7A). The contacts seem stronger than the interactions of the corresponding amine group of DRV (Fig. 7B). Analysis of the crystal structure of protease complexed with DRV had suggested that there is room

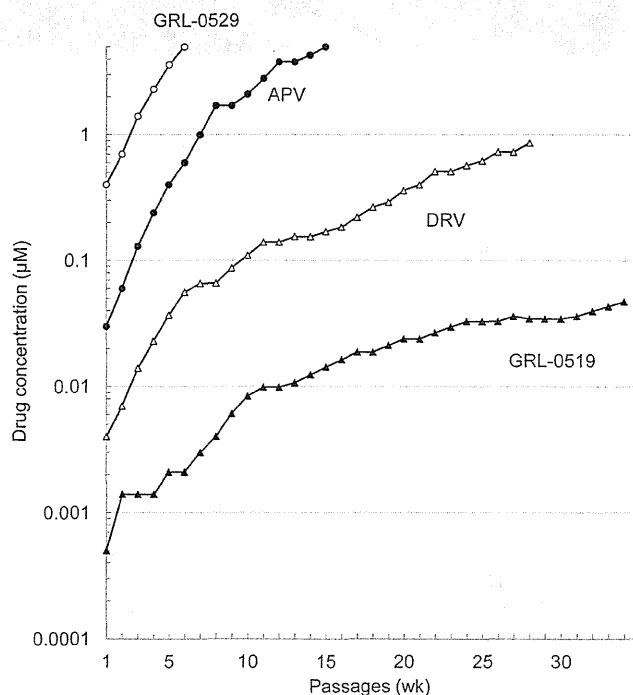


FIG 5 *In vitro* selection using a mixture of 8 multi-PI-resistant HIV-1_{MDR} isolates. A mixture of 8 different multi-PI-resistant clinical HIV-1 isolates was propagated in MT-4 cells in the presence of increasing concentrations of amprevir (●), darunavir (△), GRL-0519 (▲), or GRL-0529 (○). Each passage of virus was conducted in a cell-free manner. The amino acid substitutions identified in the protease-encoding regions of 2 different multi-PI-resistant clinical isolates compared to the consensus type B sequence cited from the Los Alamos database include L10I, I15V, E35D, N37E, K45R, I54V, L63P, A71V, V82T, L90M, I93L, and C95F in HIV-1_{MDR/A} and L10R, N37D, M46I, I62V, L63P, A71V, G73S, V77IV82T, L90M, and I93L in HIV-1_{MDR/SS}. The amino acid substitutions of the other 6 HIV-1_{MDR} variants are given in Table 3, note a.

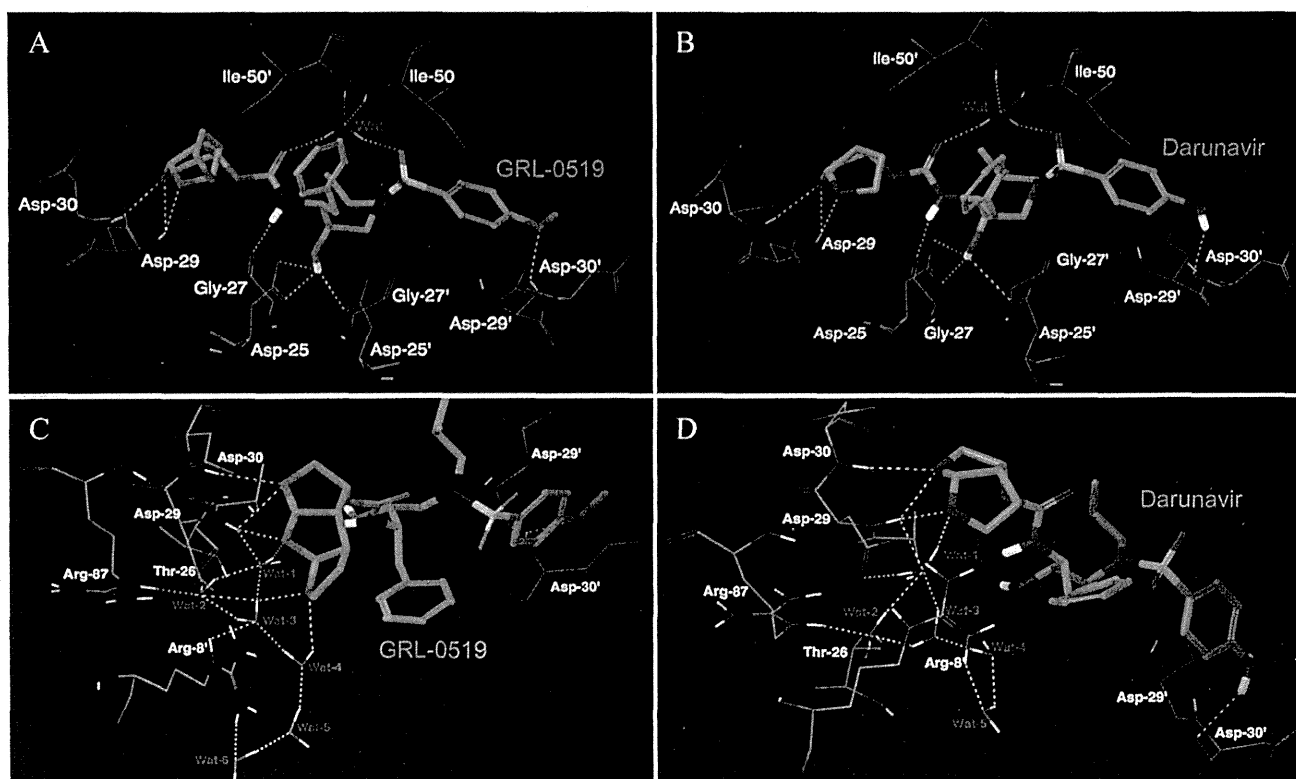


FIG 6 Hydrogen bond interactions of GRL-0519 and darunavir with protease. The interactions between protease–GRL-0519 (PDB ID, 3OK9) and protease–DRV (PDB ID, 2IEN) complexes as determined from their respective crystal structures were analyzed. (A and B) Similar interactions between protease–GRL-0519 (A) and protease–DRV (B) complexes. GRL-0519 has polar interactions with Asp-29, Asp-30, Gly-27, Asp-25, and Asp-25'. It has polar interactions with Ile-50 and Ile-50' through a bridging water molecule. The protease–DRV complex also has these polar interactions. Both inhibitors have polar interactions with different backbone atoms of Asp-30' in the S2' site of the protease. GRL-0519 interacts with the backbone amide nitrogen, whereas DRV interacts with the carbonyl oxygen. (C and D) The interactions of *tris*-THF (C) and *bis*-THF (D) moieties with water molecules highlight differences in the polar interactions of the two inhibitors. The additional THF ring of GRL-0519 interacts with an extra water molecule and has four more polar interactions than DRV. The figures shown here were made with Maestro version 9.3 (Schrödinger, LLC, New York, NY, 2012).

for an extra THF moiety to make additional contacts with protease. The crystal structure examined in the present study confirms that the *tris*-THF fully occupies the binding cavity and forms better van der Waals contacts with protease than the *bis*-THF of DRV (Fig. 7C and D). Contact (C) is defined by the following formula: $C = D_{12}/(R_1 + R_2)$, where D_{12} is the distance between atoms 1 and 2 and R_1 and R_2 are the van der Waals radii of atoms 1 and 2. A good contact is defined as follows: $1.30 > C > 0.89$.

The *tris*-THF moiety increases water-mediated polar interactions with protease. We further analyzed the polar interactions around the *tris*-THF ring of GRL-0519. The crystal structure shows that there are several water molecules that form polar interactions with GRL-0519 and bridge polar interactions with protease (Fig. 6C). Three water molecules, Wat-1, Wat-2, and Wat-3, form a tight network of hydrogen bonds among themselves and mediate polar interactions between GRL-0519 and the active-site residues. Wat-1 directly bridges the polar interactions between the oxygen of the second THF of GRL-0519 and Asp-29. The oxymethyl oxygen of the third THF ring of GRL-0519 enhances the strength of these networks of hydrogen bonds by its polar interactions with Wat-3 and Wat-4 (Fig. 6C). Wat-2 and Wat-3 also bridge the polar interaction between the oxymethyl of the third THF and Arg-87. There is one polar interaction between the third

oxymethyl and Arg-8' through Wat-3 and another network of polar interactions through Wat-4, Wat-5, and Wat-6. The crystal structure of DRV indicates the presence of five water molecules in this region compared to six present for GRL-0519 (Fig. 6D). The *tris*-THF of GRL-0519 and the additional water molecule are responsible for forming a total of 18 hydrogen bonds in this region compared to 14 for DRV, which has a *bis*-THF group as its P2 ligand.

DISCUSSION

GRL-0519, which contains a unique cyclic ether-derived nonpeptide P2 ligand, *tris*-THF, and a sulfonamide isostere, suppressed the replication of a wide spectrum of wild-type HIV-1 and HIV-2 strains with extremely low EC_{50} s (Table 1). GRL-0519 was highly potent against a variety of multidrug-resistant clinical HIV-1 isolates with EC_{50} s ranging from 0.0008 to 0.0034 μ M, while the existing FDA-approved PIs examined either failed to suppress the replication of those isolates or required much higher concentrations for viral inhibition (Table 3). GRL-0519 also efficiently blocked, with an EC_{50} of 0.03 μ M, the replications of a highly DRV-resistant variant (HIV_{DRV}^R_{P20}), to which the three PIs (APV, ATV, and LPV) had EC_{50} s of >1 μ M and DRV had an EC_{50} of 0.255 μ M (Table 3). Moreover, GRL-0519 exerted potent activity

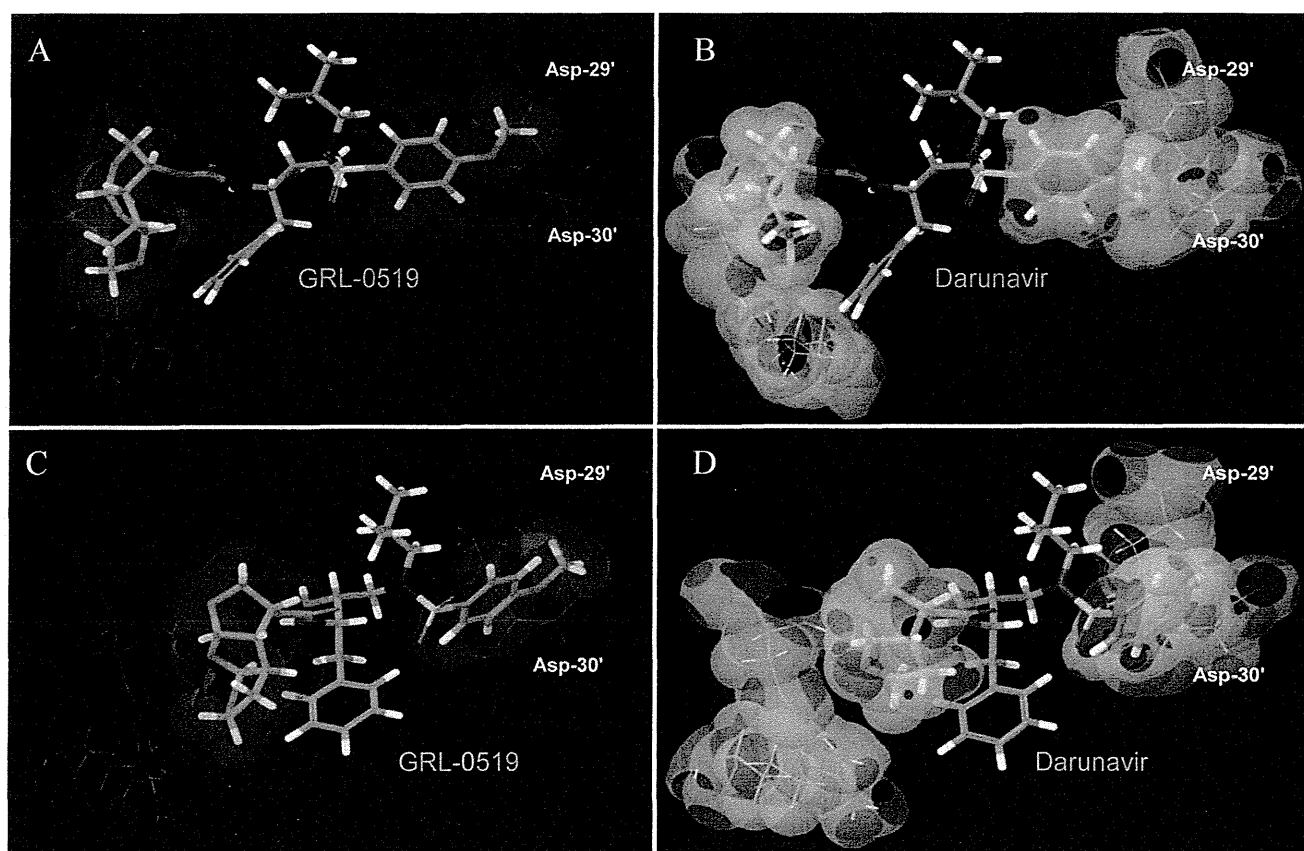


FIG 7 van der Waals interactions of GRL-0519 and darunavir with protease. GRL-0519 is shown as sticks (green carbons), and the van der Waals surfaces of selected moieties of GRL-0519 and its complexed protease are shown in gray and blue, respectively. DRV is shown as sticks (gray carbons), and the van der Waals surfaces of selected moieties of DRV and its complexed protease are shown in yellow and plum, respectively. (A and B) van der Waals interactions between the benzomethoxy of GRL-0519 and Asp-29' and Asp-30' of protease (A) and interactions between the aniline of DRV and Asp-29' and Asp-30' of protease (B). The surface interactions suggest that the methoxy group of GRL-0519 makes stronger van der Waals interactions with Asp-29' and Asp-30' of protease than does DRV. (C and D) The molecules are rotated to show the van der Waals surface interactions of the *tris*-THF (C) and *bis*-THF (D) moieties with protease. The *tris*-THF group of GRL-0519 forms better van der Waals contacts at the S2 site of protease than the *bis*-THF of DRV. The figures were made with Maestro version 9.3 (Schrödinger, LLC, New York, NY, 2012).

against laboratory PI-selected HIV-1 variants (except HIV-1_{APV}^R_{5 μ M}) with significantly low EC₅₀s (Table 2). GRL-0519 was less potent against HIV-1_{APV}^R_{5 μ M}, with an EC₅₀ of 38.0 nM (a 76-fold difference), presumably due to the structural resemblance between GRL-0519 and APV, both of which contain a sulfonamide isostere (Fig. 1).

In an attempt to explain why GRL-0519 showed such potent activity against both wild-type and drug-resistant variants, we analyzed the crystal structure of the protease–GRL-0519 complex with protease (PDB ID, 3OK9). GRL-0519 has strong polar interactions with multiple regions of protease (Fig. 6A and C). The oxygens from two of the THF rings of GRL-0519 have strong polar interactions with the backbone amide nitrogens of Asp-29 and Asp-30. GRL-0519 also forms hydrogen bonds with Gly-27 and with the side chains of the catalytic aspartates, Asp-25 and Asp-25'. The sulfonamide oxygen and the carbonyl oxygen form polar contacts with Ile-50 and Ile-50' in the flap through the bridging water molecule. Comparison of the crystal structures of protease complexes with GRL-0519 and protease complexes with DRV highlights the similarities and differences in interactions between these two inhibitors. The two oxygens from the *bis*-THF of DRV

form hydrogen bond interactions with the backbone amide nitrogens of Asp-29 and Asp-30 (Fig. 6B). DRV also forms polar interactions with Gly-27, Asp-25, and Asp-25' and polar contacts with the protease flap through the bridging water molecule. However, there are important differences in the interactions of GRL-0519 and DRV with protease. An additional water molecule (Wat-3 in Fig. 6C) around the *tris*-THF ring of GRL-0519 is observed in the crystal structure. This water molecule forms hydrogen bond interactions with the third THF ring of GRL-0519 and enhances the polar contact through a network of hydrogen bonds with Asp-29, Thr-26, Arg-87, and Arg-8'. There are four additional polar contacts arising out of the presence of the third THF ring of GRL-0519 and Wat-3 compared to the water-mediated polar interactions in this region of the protease complexes with DRV (Fig. 6D). Even though both GRL-0519 and DRV form polar interactions with the backbone atoms of Asp-30' in the S2' site, they interact with different sets of atoms (Fig. 6A and B). GRL-0519 forms the hydrogen bond with the amide nitrogen, whereas DRV forms polar contact with the carbonyl oxygen of Asp30'. The van der Waals surface interactions of GRL-0519 and DRV are also different (Fig. 7A to D). The *tris*-THF and methoxy group of GRL-0519 form

stronger van der Waals contacts with the S2 and S2' sites of protease, respectively. These interactions are stronger than the corresponding interactions of the *bis*-THF and aniline groups of DRV.

It should be noted that GRL-0519, as previously reported (35), blocks the dimerization of HIV-1 protease monomer subunits more potently, by at least 10-fold, than DRV, as examined by a fluorescence resonance energy transfer (FRET)-based HIV-1 expression assay that uses cyan (CFP) and yellow (YFP) fluorescent protein-tagged protease monomers (17). Considering that the dimerization of HIV-1 protease subunits is an essential process for its acquisition of proteolytic activity, which plays a critical role in the maturation and replication of the virus (36), the potent activity of GRL-0519 to block protease dimerization should also contribute to the greater antiviral potency of GRL-0519 than of DRV. Taken together, the stronger polar and nonpolar contacts of GRL-0519 with protease, as observed in its crystal structure, in addition to its potent activity to block protease dimerization, are likely to be responsible for its much more potent antiviral activity than that of DRV.

In our study, all the PIs examined showed no significant reduction of antiviral activity with the addition of HSA (Table 4). In contrast, the addition of AAG substantially reduced the antiretroviral activities of APV, ATV, and DRV by more than 9-fold, and their EC₅₀s increased to 286.3, 32.7, and 33.8 nM, respectively. However, the reduction with GRL-0519 was only 4-fold, and its absolute EC₅₀ was as low as 2.4 nM (Table 4). AAG is an acute-phase protein, and its concentration can increase upon injury, surgery, inflammation, malignancy, and infection, including HIV-1 infection (29, 37). Therefore, this feature of GRL-0519 may represent an advantage for its potential clinical application.

In our HIV-1_{NL4-3} selection experiment using GRL-0519, the emergence of GRL-0519-resistant variants was substantially delayed compared to other PIs and DRV. The use of a mixture of multiple-drug-resistant HIV-1 isolates can expedite the emergence of variants resistant to the drug used for the selection *in vitro* through homologous recombination and should reflect what occurs within individuals harboring a number of drug-resistant HIV-1 species (quasispecies) (28, 32). Thus, in this study, we also employed the mixture of 8 different multi-PI-resistant clinical isolates as a starting viral population (Fig. 5). In the present study, by passage 37, 3 major amino acid substitutions (K43I, A71T, and V82I) were identified in PR of HIV-1_{NL4-3}. The residue V82 is located in the vicinity of the binding pocket of the protease and forms van der Waals contact with GRL0519. The V82A substitution is reportedly associated with resistance against various protease inhibitors (33, 34). However, K43 and A71 are distal from the inhibitor binding pocket and have no direct association with GRL0519. Thus, it is likely K43I and A71T are secondary substitutions. It is particularly noteworthy that we failed to select the A28S amino acid substitution in the present selection experiment with GRL-0519. In our previous studies of potent PIs, such as TMC-126 and GRL-1398, containing a paramethoxy group in the P2' site, the A28S amino acid substitution was identified as a resistant variant (19, 25). In this regard, the combination of *tris*-THF as the P2 ligand and the paramethoxy moiety at P2' seems to have prevented the selection of the A28S substitution as a resistant variant.

The *tris*-THF moiety has more interactions with the S2 site of the protease than the *bis*-THF present in either TMC-126 or DRV. Also, the *p*-OCH₃ moiety seems to have more favorable van

der Waals interactions with the S2 site than DRV (Fig. 7). It would be reasonable to expect that the combination of *tris*-THF and *p*-OCH₃ may increase the activity, but the antiviral data suggest that GRL-0519 and TMC-126 have essentially the same antiviral activity (see Table S1 in the supplemental material). For any potential antiretroviral agents (including protease inhibitors) to exert their antiretroviral activity even *in vitro*, multiple factors are involved. They include (i) structural stability in culture medium, as well as in the cytoplasm; (ii) permeability into cells; and (iii) compartmentalization. Moreover, such potential antiretroviral agents have to tightly bind to the active site of the target viral protein (i.e., the protease active site) but should not bind to cellular proteins critical to the survival and functionality of the cells. It is possible that while GRL-0519 has greater interactions derived from the presence of the *tris*-THF group, those interactions are not directly reflected in the ultimate antiretroviral activity.

Since the GRL-0519-selected variant, HIV₅₁₉^R_{P37}, was thought to be substantially replication competent, the replication kinetics of HIV-1_{NL4-3} and HIV₅₁₉^R_{P37} were compared in the presence and absence of GRL-0519. The data showed that HIV-1_{NL4-3} failed to replicate in the presence of 0.005 μM GRL-0519 and that HIV₅₁₉^R_{P37} did the same in the presence of 0.015 μM GRL-0519 throughout the 7-day culture period (Fig. 4). The concentration range of 0.005 to 0.015 μM is relatively easily achieved in the clinical use of various PIs. For example, the peak and nadir plasma levels of DRV were ~7.1 and 3.4 μM when 400 and 100 mg of DRV/RTV were administered twice daily for 7 days (38). Considering that the EC₅₀s of GRL-0519 are extremely low, ranging from 0.0005 to 0.030 μM (Tables 1 to 4), and that GRL-0519's selectivity index of 63,714 is highly favorable compared to other conventional PIs examined in this study (Table 1), both the anti-HIV potency and safety of GRL-0519 could be favorable, although the efficacy and emergence of adverse effects should be ultimately determined by controlled clinical trials.

In conclusion, GRL-0519 possesses a number of fairly favorable features for the development of the compound as a potential therapeutic for HIV-1 infection and AIDS. However, its oral bioavailability, pharmacokinetics/pharmacodynamics, and biodistribution remain to be determined, and further investigation is warranted.

ACKNOWLEDGMENTS

This work was supported in part by a Grant for Global Education and Research Center Aiming at the Control of AIDS (Global Center of Excellence, supported by Monbu-Kagakusho); Promotion of AIDS Research from the Ministry of Health, Welfare, and Labor of Japan; a Grant to the Cooperative Research Project on Clinical and Epidemiological Studies of Emerging and Reemerging Infectious Diseases (Renkei Jigyō, no. 78; Kumamoto University) of Monbu-Kagakusho (H.M.); the Intramural Research Program of the Center for Cancer Research, National Cancer Institute, National Institutes of Health (H.M.); and by a grant from the National Institutes of Health (GM53386; A.K.G.).

REFERENCES

- Edmonds A, Yotebieng M, Lusiana J, Matumona Y, Kiteetele F, Napravnik S, Cole SR, Van Rie A, Behets F. 2011. The effect of highly active antiretroviral therapy on the survival of HIV-infected children in a resource-deprived setting: a cohort study. *PLoS Med.* 8:e1001044. doi:10.1371/journal.pmed.1001044.
- Lohse N, Hansen AB, Gerstoft J, Obel N. 2007. Improved survival in HIV-infected persons: consequences and perspectives. *J. Antimicrob. Chemother.* 60:461–463.

3. Mitsuya H, Maeda K, Das D, Ghosh AK. 2008. Development of protease inhibitors and the fight with drug-resistant HIV-1 variants. *Adv. Pharmacol.* 56:169–197.
4. Walensky RP, Paltiel AD, Losina E, Mercincavage LM, Schackman BR, Sax PE, Weinstein MC, Freedberg KA. 2006. The survival benefits of AIDS treatment in the United States. *J. Infect. Dis.* 194:11–19.
5. De Clercq E. 2002. Strategies in the design of antiviral drugs. *Nat. Rev. Drug Discov.* 1:13–25.
6. Siliciano JD, Siliciano RF. 2004. A long-term latent reservoir for HIV-1. *J. Antimicrob. Chemother.* 54:6–9.
7. Simon V, Ho DD. 2003. HIV-1 dynamics in vivo: implications for therapy. *Nat. Rev. Microbiol.* 1:181–190.
8. Carr A. 2003. Toxicity of antiretroviral therapy and implications for drug development. *Nat. Rev. Drug Discov.* 2:624–634.
9. Fumero E, Podzamczar D. 2003. New patterns of HIV-1 resistance during HAART. *Clin. Microbiol. Infect.* 9:1077–1084.
10. Grabar S, Weiss L, Costagliola D. 2006. HIV infection in older patients in the HAART era. *J. Antimicrob. Chemother.* 57:4–7.
11. Hirsch HH, Kaufmann G, Sendi P, Bategay M. 2004. Immune reconstitution in HIV-infected patients. *Clin. Infect. Dis.* 38:1159–1166.
12. Little SJ, Holte S, Routy JP, Daar ES, Markowitz M, Collier AC, Koup RA, Mellors JW, Connick E, Conway B, Kilby M, Wang L, Whitcomb JM, Hellmann NS, Richman DD. 2002. Antiretroviral-drug resistance among patients recently infected with HIV. *N. Engl. J. Med.* 347:385–394.
13. Naggie S, Hicks C. 2010. Protease inhibitor-based antiretroviral therapy in treatment-naïve HIV-1-infected patients: the evidence behind the options. *J. Antimicrob. Chemother.* 65:1094–1099.
14. Ghosh AK, Kincaid JF, Cho W, Walters DE, Krishnan K, Hussain KA, Koo Y, Cho H, Rudall C, Holland L, Buthod J. 1998. Potent HIV protease inhibitors incorporating high-affinity P2-ligands and (R)-(hydroxyethylamino)sulfonamide isostere. *Bioorg. Med. Chem. Lett.* 8:687–690.
15. Ghosh AK, Krishnan K, Walters DE, Cho W, Cho H, Koo Y, Trevino J, Holland L, Buthod J. 1998. Structure based design: novel spirocyclic ethers as nonpeptidic P2-ligands for HIV protease inhibitors. *Bioorg. Med. Chem. Lett.* 8:979–982.
16. Koh Y, Nakata H, Maeda K, Ogata H, Bilcer G, Devasamudram T, Kincaid JF, Boross P, Wang YF, Tie Y, Volarath P, Gaddis L, Harrison RW, Weber IT, Ghosh AK, Mitsuya H. 2003. Novel bis-tetrahydrofuranylethane-containing nonpeptidic protease inhibitor (PI) UIC-94017 (TMC114) with potent activity against multi-PI-resistant human immunodeficiency virus in vitro. *Antimicrob. Agents Chemother.* 47:3123–3129.
17. Ghosh AK, Xu CX, Rao KV, Baldrige A, Agniswamy J, Wang YF, Weber IT, Aoki M, Miguel SG, Amano M, Mitsuya H. 2010. Probing multidrug-resistance and protein-ligand interactions with oxatricyclic designed ligands in HIV-1 protease inhibitors. *ChemMedChem* 5:1850–1854.
18. Shirasaka T, Kavlick MF, Ueno T, Gao WY, Kojima E, Alcaide ML, Chokekijchai S, Roy BM, Arnold E, Yarchoan R, Mitsuya H. 1995. Emergence of human immunodeficiency virus type 1 variants with resistance to multiple dideoxynucleosides in patients receiving therapy with dideoxynucleosides. *Proc. Natl. Acad. Sci. U. S. A.* 92:2398–2402.
19. Yoshimura K, Kato R, Kavlick MF, Nguyen A, Maroun V, Maeda K, Hussain KA, Ghosh AK, Gulnik SV, Erickson JW, Mitsuya H. 2002. A potent human immunodeficiency virus type 1 protease inhibitor, UIC-94003 (TMC-126), and selection of a novel (A28S) mutation in the protease active site. *J. Virol.* 76:1349–1358.
20. Yoshimura K, Kato R, Yusa K, Kavlick MF, Maroun V, Nguyen A, Mimoto T, Ueno T, Shintani M, Falloon J, Masur H, Hayashi H, Erickson J, Mitsuya H. 1999. JE-2147: a dipeptide protease inhibitor (PI) that potently inhibits multi-PI-resistant HIV-1. *Proc. Natl. Acad. Sci. U. S. A.* 96:8675–8680.
21. Ghosh AK, Leshchenko S, Noetzel M. 2004. Stereoselective photochemical 1,3-dioxolane addition to 5-alkoxymethyl-2(5H)-furanone: synthesis of bis-tetrahydrofuranil ligand for HIV protease inhibitor UIC-94017 (TMC-114). *J. Org. Chem.* 69:7822–7829.
22. Maeda K, Yoshimura K, Shibayama S, Habashita H, Tada H, Sagawa K, Miyakawa T, Aoki M, Fukushima D, Mitsuya H. 2001. Novel low molecular weight spirodiketopiperazine derivatives potently inhibit R5 HIV-1 infection through their antagonistic effects on CCR5. *J. Biol. Chem.* 276:35194–35200.
23. Nakata H, Amano M, Koh Y, Kodama E, Yang G, Bailey CM, Kohgo S, Hayakawa H, Matsuoka M, Anderson KS, Cheng YC, Mitsuya H. 2007. Activity against human immunodeficiency virus type 1, intracellular metabolism, and effects on human DNA polymerases of 4'-ethynyl-2-fluoro-2'-deoxyadenosine. *Antimicrob. Agents Chemother.* 51:2701–2708.
24. Amano M, Koh Y, Das D, Li J, Leschenko S, Wang YF, Boross PI, Weber IT, Ghosh AK, Mitsuya H. 2007. A novel bis-tetrahydrofuranylethane-containing nonpeptidic protease inhibitor (PI), GRL-98065, is potent against multiple-PI-resistant human immunodeficiency virus in vitro. *Antimicrob. Agents Chemother.* 51:2143–2155.
25. Ide K, Aoki M, Amano M, Koh Y, Yedidi RS, Das D, Leschenko S, Chapsal B, Ghosh AK, Mitsuya H. 2011. Novel HIV-1 protease inhibitors (PIs) containing a bicyclic P2 functional moiety, tetrahydroprano-tetrahydrofuran, that are potent against multi-PI-resistant HIV-1 variants. *Antimicrob. Agents Chemother.* 55:1717–1727.
26. Tojo Y, Koh Y, Amano M, Aoki M, Das D, Kulkarni S, Anderson DD, Ghosh AK, Mitsuya H. 2010. Novel protease inhibitors (PIs) containing macrocyclic components and 3(R),3a(S),6a(R)-bis-tetrahydrofuranylethane that are potent against multi-PI-resistant HIV-1 variants in vitro. *Antimicrob. Agents Chemother.* 54:3460–3470.
27. Kaminski GA, Friesner EA. 2001. Evaluation and reparametrization of the OPLS-AA force field for proteins via comparison with accurate quantum chemical calculations on peptides. *J. Phys. Chem. B* 105:6474–6487.
28. Koh Y, Amano M, Towata T, Danish M, Leshchenko-Yashchuk S, Das D, Nakayama M, Tojo Y, Ghosh AK, Mitsuya H. 2010. In vitro selection of highly darunavir-resistant and replication-competent HIV-1 variants by using a mixture of clinical HIV-1 isolates resistant to multiple conventional protease inhibitors. *J. Virol.* 84:11961–11969.
29. Schon A, Ingaramo M, Freire E. 2003. The binding of HIV-1 protease inhibitors to human serum proteins. *Biophys. Chem.* 105:221–230.
30. Marcelin AG, Affolabi D, Lamotte C, Mohand HA, Delaugerre C, Wirden M, Voujon D, Bossi P, Ktorza N, Bricaire F, Costagliola D, Katlama C, Peytavin G, Calvez V. 2004. Resistance profiles observed in virological failures after 24 weeks of amprenavir/ritonavir containing regimen in protease inhibitor experienced patients. *J. Med. Virol.* 74:16–20.
31. Young TP, Parkin NT, Stawiski E, Pilot-Matias T, Trinh R, Kempf DJ, Norton M. 2010. Prevalence, mutation patterns, and effects on protease inhibitor susceptibility of the L76V mutation in HIV-1 protease. *Antimicrob. Agents Chemother.* 54:4903–4906.
32. Aoki M, Danish ML, Aoki-Ogata H, Amano M, Ide K, Koh Y, Mitsuya H. 2012. The loss of protease dimerization inhibition activity of tipranavir (TPV) and its association with HIV-1 acquisition of resistance to TPV. *J. Virol.* 86:13384–13396.
33. Wlodawer A, Vondrasek J. 1998. Inhibitors of HIV-1 protease: a major success of structure-assisted drug design. *Annu. Rev. Biophys. Biomol. Struct.* 27:249–284.
34. Wlodawer A, Erickson JW. 1993. Structure-based inhibitors of HIV-1 protease. *Annu. Rev. Biochem.* 62:543–585.
35. Koh Y, Matsumi S, Das D, Amano M, Davis DA, Li J, Leschenko S, Baldrige A, Shioda T, Yarchoan R, Ghosh AK, Mitsuya H. 2007. Potent inhibition of HIV-1 replication by novel non-peptidyl small molecule inhibitors of protease dimerization. *J. Biol. Chem.* 282:28709–28720.
36. Dunn BM, Goodenow MM, Gustchina A, Wlodawer A. 2002. Retroviral proteases. *Genome Biol.* 3:reviews3006.1-reviews3006.7. doi:10.1186/gb-2002-3-4-reviews3006.
37. Fournier T, Medjoubi NN, Porquet D. 2000. Alpha-1-acid glycoprotein. *Biochim. Biophys. Acta* 1482:157–171.
38. Boffito M, Miralles D, Hill A. 2008. Pharmacokinetics, efficacy, and safety of darunavir/ritonavir 800/100 mg once-daily in treatment-naïve and -experienced patients. *HIV Clin. Trials* 9:418–427.

Loss of the Protease Dimerization Inhibition Activity of Tipranavir (TPV) and Its Association with the Acquisition of Resistance to TPV by HIV-1

Manabu Aoki,^{a,b} Matthew L. Danish,^a Hiromi Aoki-Ogata,^a Masayuki Amano,^a Kazuhiko Ide,^a Debananda Das,^c Yasuhiro Koh,^a and Hiroaki Mitsuya^{a,c}

Departments of Infectious Diseases and Hematology, Kumamoto University Graduate School of Medical Sciences, Kumamoto, Japan^a; Department of Medical Technology, Kumamoto Health Science University, Kumamoto, Japan^b; and Experimental Retrovirology Section, HIV and AIDS Malignancy Branch, National Cancer Institute, National Institutes of Health, Bethesda, Maryland, USA^c

Tipranavir (TPV), a protease inhibitor (PI) inhibiting the enzymatic activity and dimerization of HIV-1 protease, exerts potent activity against multi-PI-resistant HIV-1 isolates. When a mixture of 11 multi-PI-resistant (but TPV-sensitive) clinical isolates (HIV_{11MIX}), which included HIV_B and HIV_C, was selected against TPV, HIV_{11MIX} rapidly (by 10 passages [HIV_{11MIX}^{P10}]) acquired high-level TPV resistance and replicated at high concentrations of TPV. HIV_{11MIX}^{P10} contained various amino acid substitutions, including I54V and V82T. The intermolecular FRET-based HIV-1 expression assay revealed that TPV's dimerization inhibition activity against cloned HIV_B (cHIV_B) was substantially compromised. The introduction of I54V/V82T into wild-type cHIV_{NL4-3} (cHIV_{NL4-3}^{I54V/V82T}) did not block TPV's dimerization inhibition or confer TPV resistance. However, the introduction of I54V/V82T into cHIV_B (cHIV_B^{I54V/V82T}) compromised TPV's dimerization inhibition and cHIV_B^{I54V/V82T} proved to be significantly TPV resistant. L24M was responsible for TPV resistance with the cHIV_C genetic background. The introduction of L24M into cHIV_{NL4-3} (cHIV_{NL4-3}^{L24M}) interfered with TPV's dimerization inhibition, while L24M increased HIV-1's susceptibility to TPV with the HIV_{NL4-3} genetic background. When selected with TPV, cHIV_{NL4-3}^{I54V/V82T} most readily developed TPV resistance and acquired E34D, which compromised TPV's dimerization inhibition with the HIV_{NL4-3} genetic background. The present data demonstrate that certain amino acid substitutions compromise TPV's dimerization inhibition and confer TPV resistance, although the loss of TPV's dimerization inhibition is not always associated with significantly increased TPV resistance. The findings that TPV's dimerization inhibition is compromised with one or two amino acid substitutions may explain at least in part why the genetic barrier of TPV against HIV-1's development of TPV resistance is relatively low compared to that of darunavir.

Tipranavir (TPV) is a nonpeptidyl protease (PR) inhibitor (PI) which is administered in combination antiretroviral therapy to treat HIV-1 infection and AIDS. TPV has been shown to inhibit the replication of HIV-1 variants that are resistant to other PIs and is recommended for patients who harbor multi-PI-resistant HIV-1 variants and do not respond to therapeutic regimens, including PIs (34). HIV-1 resistance to TPV has been reported to require multiple amino acid substitutions in protease (9); however, we have witnessed that HIV-1 often acquires significant levels of resistance to TPV among HIV-1-infected individuals receiving long-term combination chemotherapy (4, 17, 31). TPV is currently not recommended in the initial therapy mainly because of the higher rate at which patients previously experienced hepatic abnormalities (5, 29, 37).

Dimerization of HIV-1 PR subunits is an essential process for the acquisition of the proteolytic activity of HIV-1 PR (23, 39). Thus, inhibition of PR dimerization likely abolishes proteolytic activity and intervenes in the replication of HIV-1. We have recently developed an intermolecular fluorescence resonance energy transfer (FRET)-based HIV-1 expression assay employing cyan fluorescent protein (CFP)- and yellow fluorescent protein (YFP)-tagged HIV-1 PR monomers to detect and quantify PR dimerization (21). Using this assay, we have recently identified a group of nonpeptidyl small-molecule inhibitors of HIV-1 PR dimerization, including TPV, darunavir (DRV), and a series of experimental antiretroviral agents (21). DRV (12, 13, 22) potentially inhibits the enzymatic activity and dimerization of HIV-1 PR (20,

21), and a high genetic barrier against HIV-1 development of DRV resistance exists (7, 8). However, various amino acid substitutions that are potentially related to HIV-1 resistance to DRV have been reported (7, 19, 20, 27, 38). We have recently demonstrated, using the FRET-based HIV-1 expression assay, that the loss of DRV activity to inhibit protease dimerization requires at least four combined amino acid substitutions in protease and that the loss of DRV's protease dimerization inhibition activity is associated with HIV-1 acquisition of DRV resistance (20). In the present work, we specifically asked whether TPV's protease dimerization inhibition activity contributes to the antiretroviral activity of TPV against a series of multi-PI-resistant HIV-1 variants and whether the loss of such protease dimerization inhibition activity of TPV is associated with the development of HIV-1 resistance to TPV.

MATERIALS AND METHODS

Cells and viruses. MT-4 cells were grown in RPMI 1640-based culture medium, while 293T and COS7 cells were propagated in Dulbecco's mod-

Received 29 December 2011 Accepted 20 September 2012

Published ahead of print 26 September 2012

Address correspondence to Hiroaki Mitsuya, hmitsuya@helix.nih.gov.

Supplemental material for this article may be found at <http://jvi.asm.org/>.

Copyright © 2012, American Society for Microbiology. All Rights Reserved.

doi:10.1128/JVI.07234-11

ified Eagle's medium. These media were supplemented with 10% fetal calf serum (FCS; PAA Laboratories GmbH, Linz, Austria) plus 50 U of penicillin and 50 µg of kanamycin per ml. Peripheral blood mononuclear cells (PBMCs) were isolated from the buffy coat of HIV-1-seronegative individuals using Ficoll-Hypaque density gradient centrifugation and cultured in RPMI 1640-based culture medium containing 10% FCS and antibiotics with 10 µg of phytohemagglutinin (PHA-PBMCs) for 3 days prior to use. The following HIV-1 strains were used for the drug susceptibility assay and selection experiments: a clinical HIV-1 strain isolated from an antiretroviral therapy-naïve patients with AIDS (HIV_{104pre}) (41) and 11 HIV-1 clinical strains (HIV_A, HIV_B, HIV_C, HIV_G, HIV_{1M}, HIV_{MM}, HIV_{JSL}, HIV_{SS}, HIV_{ES}, HIV_{EV}, and HIV₁₃₋₅₂) which were originally isolated from patients with AIDS who were enrolled in an open-label clinical study of amprenavir (APV) and abacavir (ABC) at the Clinical Center, National Institutes of Health, and were randomly chosen from among the enrollees who had failed the APV-plus-ABC therapy (36, 41) or a phase I/II study of tenofovir disoproxil fumarate (TDF) (15). Such patients had failed existing anti-HIV-1 regimens after receiving 7 to 11 anti-HIV-1 drugs over the previous 24 to 83 months in the 1990s (15, 36, 41). The clinical strains used in the present study contained 8 to 16 amino acid substitutions in the protease-encoding region which have reportedly

been associated with HIV-1 resistance to various PIs and have been genotypically and phenotypically characterized as multi-PI-resistant HIV-1. The amino acid sequences of the protease of the 11 clinical isolates are illustrated in Fig. S1 in the supplemental material.

Antiviral agents. DRV was synthesized as described previously (14). Saquinavir (SQV) was kindly provided by Roche Products Ltd. (Welwyn Garden City, United Kingdom) and Abbott Laboratories (Abbott Park, IL). APV was a kind gift from GlaxoSmithKline (Research Triangle Park, N.C.). Indinavir (IDV) and lopinavir (LPV) were kindly provided by Japan Energy Inc., Tokyo, Japan. Atazanavir (ATV) was a kind gift from Bristol-Myers Squibb (New York, NY). TPV was obtained through the AIDS Research and Reference Reagent Program, Division of AIDS, NIAID, National Institutes of Health.

Generation of highly TPV-resistant HIV-1 *in vitro*. Thirty 50% tissue culture infectious doses (TCID₅₀s) of each of the 11 highly multi-PI-resistant HIV-1 isolates was mixed and propagated in a mixture of an equal number of PHA-PBMCs (5×10^5) and MT-4 cells (5×10^5), in an attempt to adapt them for replication in MT-4 cells. The cell-free supernatant was harvested on day 7 of coculture (PHA-PBMCs and MT-4 cells), and the viruses (designated HIV_{11MIX}^{P0}, where P0 represents passage 0) were further propagated in fresh MT-4 cells for the selection experiment (19). On the first passage, MT-4 cells (5×10^5) were exposed to culture supernatant of mixed viruses or 500 TCID₅₀s of each infectious molecular HIV-1 clone and cultured in the presence of TPV at initial concentrations of 0.1 to 0.4 µM. On the last day of each passage (approximately day 7), 1 ml of the cell-free supernatant was harvested and transferred to a culture of fresh uninfected MT-4 cells in the presence of increased concentrations of the drug for the following round of culture. In this round of culture, three drug concentrations (increased by 1-, 2-, and 3-fold compared to the previous concentration) were employed. When the replication of HIV-1 in the culture was confirmed by substantial Gag protein production (greater than 200 ng/ml), the highest drug concentration among the three concentrations was used to continue the selection (for the next round of culture). This protocol was repetitively used until the drug concentration reached the targeted concentration (2, 19). Proviral DNA samples obtained from the lysates of infected cells were subjected to nucleotide sequencing.

Determination of nucleotide sequences. Molecular cloning and determination of the nucleotide sequences of HIV-1 strains passaged in the presence of TPV were performed as previously described (2, 40). In brief, high-molecular-weight DNA was extracted from HIV-1-infected MT-4 cells by using the InstaGene matrix (Bio-Rad Laboratories, Hercules, CA) and was subjected to molecular cloning, followed by sequence determination. The primers used for the first round of PCR with the entire Gag-

and protease-encoding regions of the HIV-1 genome were LTR F1 (5'-GAT GCT ACA TAT AAG CAG CTG C-3') and PRI2 (5'-CTC GTG ACA AAT TTC TAC TAA TGC-3'). The first-round PCR mixture consisted of 1 µl of proviral DNA solution, 10 µl of Premix Taq (ExTaq version; TaKaRa Bio Inc., Otsu, Japan), and 10 pmol of each of the first PCR primers in a total volume of 20 µl. The PCR conditions used were an initial 3 min at 95°C, followed by 30 cycles of 40 s at 95°C, 20 s at 55°C, and 2 min at 72°C, with a final 10 min of extension at 72°C. The first-round PCR products (1 µl) were used directly in the second round of PCR with primers LTR F2 (5'-GAG ACT CTG GTA ACT AGA GAT C-3') and Ksm2.1 (5'-CCA TCC CGG GCT TTA ATT TTA CTG GTA C-3') under the PCR conditions of an initial 3 min at 95°C, followed by 30 cycles of 30 s at 95°C, 20 s at 55°C, and 2 min at 72°C, with a final 10 min of extension at 72°C. The second-round PCR products were purified with spin columns (MicroSpin S-400 HR columns; Amersham Biosciences Corp., Piscataway, NJ), cloned directly, and subjected to sequencing with a model 3130 automated DNA sequencer (Applied Biosystems, Foster City, CA).

Drug susceptibility assay. To determine the susceptibility of HIV_{104pre} and clinical multi-PI-resistant HIV-1 isolates, PHA-PBMCs (10⁶/ml) were exposed to 50 TCID₅₀s of each HIV-1 isolate and cultured in the presence or absence of various concentrations of drugs in 10-fold serial dilutions in 96-well microtiter culture plates. PHA-PBMCs were derived from a single donor in each independent experiment. For obtaining the data, three different donors were recruited. To determine the drug susceptibility of infectious molecular HIV-1 clones and TPV-selected HIV-1 variants, MT-4 cells were used as target cells. MT-4 cells (10⁵/ml) were exposed to 50 TCID₅₀s of infectious molecular HIV-1 clones and TPV-selected HIV-1 variants in the presence or absence of various concentrations of drugs and were incubated at 37°C. On day 7 of culture, the supernatant was harvested and the amount of p24 Gag protein was determined by using a fully automated chemiluminescent enzyme immunoassay system (Lumipulse F; Fujirebio Inc., Tokyo, Japan) (22). The drug concentrations that suppressed the production of p24 Gag protein by 50% (50% inhibitory concentrations [IC₅₀s]) were determined by comparison with the level of p24 production in drug-free control cell cultures. All assays were performed in duplicate or triplicate (1, 18, 22).

Generation of recombinant HIV-1 clones. The PCR products obtained as described above were digested with two of the three enzymes BssHII, ApaI, and XmaI, and the obtained fragments were introduced into pHIV-1_{NLSma}, designed to have a SmaI site by changing two nucleotides (2590 and 2593) of pHIV-1_{NL4-3} (2, 11). To generate HIV-1 clones carrying the mutations, site-directed mutagenesis was performed using a QuikChange site-directed mutagenesis kit (Stratagene, La Jolla, CA), and the mutation-containing genomic fragments were introduced into pHIV-1_{NLSma}. Determination of the nucleotide sequences of plasmids confirmed that each clone had the desired mutations but no unintended mutations. 293T cells were transfected with each recombinant plasmid by using Lipofectamine 2000 reagent (Invitrogen, Carlsbad, CA), and the infectious virions thus obtained were harvested 48 h after transfection and stored at -80°C until use.

Generation of FRET-based HIV-1 expression system. The intermolecular fluorescence resonance energy transfer-based HIV-1 expression assay employing cyan and yellow fluorescent protein (CFP and YFP, respectively)-tagged protease monomers was generated as previously described (Fig. 1) (21). In brief, CFP- and YFP-tagged wild-type HIV-1 protease constructs (pHIV-PR_{WT}^{CFP} and pHIV-PR_{WT}^{YFP}, respectively) were generated using BD Creator DNA cloning kits (BD Biosciences, San Jose, CA). For the generation of full-length molecular infectious clones containing CFP- or YFP-tagged protease, the PCR-mediated recombination method was used (10). A linker consisting of five alanines was inserted between protease and fluorescent proteins. The phenylalanine-proline site that HIV-1 protease cleaves was also introduced between the fluorescent protein and reverse transcriptase (RT). DNA fragments thus obtained were subsequently joined by using the PCR-mediated recombination reaction performed under the standard conditions for ExTaq poly-

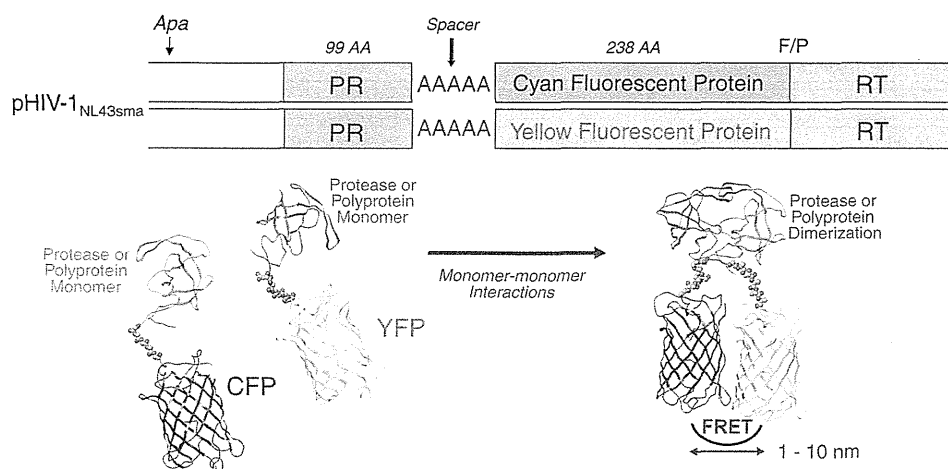


FIG 1 FRET-based HIV expression system. Plasmids encoding full-length molecular infectious HIV (HIV_{NL4-3}) clones that produce CFP- or YFP-tagged PR were prepared using the PCR-mediated recombination method, as described in Materials and Methods. A linker consisting of five alanines was inserted between HIV PR and the fluorescent protein. A phenylalanine-proline site (F/P) that HIV PR cleaves was introduced between the fluorescent protein and RT. Shown are structural representations of PR monomers and dimer in association with the linker atoms and fluorescent proteins. FRET occurs when the two fluorescent proteins become 1 to 10 nm apart. If an agent that is capable of inhibiting the dimerization of PR monomer subunits is present when the CFP- and YFP-tagged PR monomers are produced within the cell upon cotransfection, no FRET occurs.

merase (TaKaRa Bio Inc., Otsu, Japan). The amplified PCR products were cloned into the pCR-XL-TOPO vector according to the manufacturer's instructions (Gateway cloning system; Invitrogen, Carlsbad, CA). PCR products were generated with the pCR-XL-TOPO vector as the templates, followed by digestion by both *ApaI* and *XmaI*, and the *ApaI*-*XmaI* fragment was introduced into pHIV-1_{NLSma} (11), generating pHIV-PR_{WT}^{CFP} and pHIV-PR_{WT}^{YFP}, respectively.

FRET procedure. COS7 cells plated on an EZ view cover-glass-bottom culture plate (Iwaki, Tokyo, Japan) were transfected with pHIV-PR_{WT}^{CFP} and pHIV-PR_{WT}^{YFP} using Lipofectamine 2000 (Invitrogen, Carlsbad, CA) according to the manufacturer's instructions in the presence of various concentrations of each compound, cultured for 72 h, and analyzed under a Fluoview FV500 confocal laser scanning microscope (Olympus Optical Corp., Tokyo, Japan) at room temperature as previously described (21). When the effect of each compound was analyzed by FRET, test compounds were added to the culture medium simultaneously with plasmid transfection. Results of FRET were determined by quenching of CFP (donor) fluorescence and an increase in YFP (acceptor) fluorescence (sensitized emission), since part of the energy of CFP is transferred to YFP instead of being emitted. The changes in the CFP and YFP fluorescence intensity in the images of selected regions were examined and quantified using the Olympus FV500 Image software system (Olympus Optical Corp). Background values were obtained from the regions where no cells were present and were subtracted from the values for the cells examined in all calculations. Ratios of intensities of CFP fluorescence after photobleaching to CFP fluorescence prior to photobleaching (CFP^{A/B} ratios) were determined. It is well established that CFP^{A/B} ratios of greater than 1.0 indicate that an association of CFP- and YFP-tagged proteins occurred, and it was interpreted that the dimerization of protease subunits occurred. CFP^{A/B} ratios of less than 1 indicated that the association of the two subunits did not occur, and it was interpreted that protease dimerization was inhibited (21).

RESULTS

Generation of TPV-resistant HIV-1 using a mixture of multi-PI-resistant clinical HIV-1 isolates. TPV and DRV inhibit the enzymatic activity of HIV-1 protease (21, 30), block the dimerization of protease subunits (21), and exert potent activity against a wide spectrum of wild-type and multi-PI-resistant HIV-1 variants (3,

22, 30). Although the emergence of DRV-resistant HIV-1 is substantially delayed *in vitro* (6, 19) and *in vivo* (32), we recently reported that the use of a mixture of 8 multiple-PI-resistant clinical HIV-1 isolates as a starting HIV-1 population makes it possible to relatively rapidly select highly DRV-resistant HIV-1 variants (19). We therefore attempted to generate TPV-resistant HIV-1 variants, employing as a starting HIV-1 population a mixture of 11 highly multiple-PI-resistant clinical HIV-1 strains (HIV_{11MIX}) isolated from patients with AIDS, who had failed multiple antiretroviral regimens containing various PIs. All such clinical isolates contained a variety of PI resistance-associated amino acid substitutions in their protease and showed, in general, high levels of resistance to five approved PIs (SQV, IDV, APV, LPV, and ATV), as examined in PHA-PBMCs as target cells using p24 production inhibition as an endpoint (Table 1). However, it was noted that TPV retained its anti-HIV-1 activity against each of the virus strains in HIV_{11MIX}, with 0.4- to 3-fold-differences in its IC₅₀ against a wild-type clinical strain HIV_{104pre} (35) relative to those against multiple-PI-resistant clinical HIV-1 strains (Table 1).

Each of four selected primary strains (HIV_B, HIV_C, HIV_G, and HIV_{TM}) and HIV_{11MIX} were propagated in a mixture of an equal number of PHA-PBMCs and MT-4 cells, in an attempt to adapt each virus population for replication in MT-4 cells in the presence of 0.4 μM TPV as a starting concentration. The four primary HIV-1 strains were chosen since they were all highly resistant to the majority of nucleoside reverse transcriptase inhibitors (35, 41) and a variety of PIs (Table 1). The cell-free supernatant was harvested at the conclusion of each passage (approximately 7 days) of culture, and the viral preparation was further propagated in fresh MT-4 cells. HIV_{11MIX} at passage 10 (HIV_{11MIX}^{P10}) was capable of replicating in the presence of TPV at a concentration as high as 15 μM (Fig. 2). Two (HIV_B and HIV_C) of the four primary HIV strains also became replicative in the presence of 15 μM TPV by passages 10 and 15, respectively, while HIV_G and HIV_{TM} failed to replicate in the presence of 2 and 3 μM TPV, respectively (Fig. 2). However, the HIV_{NL4-3} clone (cHIV_{NL4-3}) did not develop a high

TABLE 1 Sensitivities of multidrug-resistant clinical isolates to various PIs^a

Virus	IC ₅₀ ^a mean ± SD (μM) (fold change)					
	SQV	IDV	APV	LPV	ATV	TPV
HIV _{104pre}	0.0073 ± 0.0014	0.042 ± 0.003	0.029 ± 0.002	0.034 ± 0.002	0.002 ± 0.0004	0.16 ± 0.03
HIV _A	0.075 ± 0.001 (10)	0.59 ± 0.04 (14)	0.074 ± 0.013 (3)	0.26 ± 0.014 (8)	0.024 ± 0.003 (12)	0.36 ± 0.007 (2)
HIV _B	0.36 ± 0.001 (49)	>1 (>24)	>1 (>34)	>1 (>29)	0.28 ± 0.01 (140)	0.18 ± 0.01 (1)
HIV _C	0.032 ± 0.002 (4)	>1 (>24)	0.37 ± 0.01 (11)	>1 (>29)	0.034 ± 0.004 (17)	0.17 ± 0.04 (1)
HIV _G	0.030 ± 0.001 (4)	0.36 ± 0.1 (9)	0.43 ± 0.04 (15)	0.26 ± 0.04 (8)	0.043 ± 0.022 (22)	0.24 ± 0.08 (2)
HIV _{TM}	0.26 ± 0.04 (36)	>1 (>24)	0.32 ± 0.007 (11)	>1 (>29)	0.065 ± 0.008 (33)	0.38 ± 0.05 (2)
HIV _{MM}	0.22 ± 0.01 (29)	>1 (>24)	0.32 ± 0.03 (11)	0.59 ± 0.004 (17)	0.21 ± 0.02 (105)	0.35 ± 0.007 (2)
HIV _{SS}	0.17 ± 0.004 (23)	>1 (>24)	0.13 ± 0.01 (4)	0.21 ± 0.04 (6)	0.032 ± 0.006 (16)	0.41 ± 0.14 (3)
HIV _{ISL}	0.30 ± 0.02 (41)	>1 (>24)	0.78 ± 0.1 (27)	>1 (>29)	0.43 ± 0.04 (215)	0.23 ± 0.05 (1)
HIV _{EV}	0.36 ± 0.05 (49)	0.25 ± 0.02 (6)	>1 (>34)	>1 (>29)	0.43 ± 0.04 (215)	0.066 ± 0.016 (0.4)
HIV _{ES}	0.45 ± 0.01 (62)	>1 (>24)	>1 (>34)	0.41 ± 0.01 (12)	0.032 ± 0.004 (16)	0.34 ± 0.01 (2)
HIV ₁₃₋₅₂	0.029 ± 0.003 (4)	0.32 ± 0.03 (7)	0.030 ± 0.003 (1)	0.22 ± 0.1 (6)	0.021 ± 0.007 (11)	0.10 ± 0.01 (0.6)

^a IC₅₀s were determined by using PHA-PBMCs as target cells, and the inhibition of p24 Gag protein production by each drug was used as the endpoint. Numbers in parentheses represent the *n*-fold change of the IC₅₀ for each isolate compared to the IC₅₀ for wild-type strain HIV_{104pre}. All assays were conducted in duplicate or triplicate, and the data shown represent mean values ± 1 standard deviation derived from the results of three independent experiments. PHA-PBMCs were derived from a single donor in each independent experiment.

level of resistance to TPV, and its replication was found to be significantly compromised in the presence of >1.5 μM TPV (Fig. 2).

Susceptibility of TPV-selected HIV_{11MIX} populations to various PIs, including TPV. In order to determine the susceptibility of the above-described TPV-selected HIV-1 variants to seven FDA-approved PIs, we harvested HIV_{11MIX}^{P0}, HIV_{11MIX}^{P5}, and HIV_{11MIX}^{P10} at passages 0, 5, and 10, respectively, and tested them using the drug susceptibility assay. As shown in Table 2, HIV_{11MIX}^{P0} showed considerable resistance to 5 PIs (SQV, IDV, APV, LPV, and ATV), with fold changes of 8 to 29 in their IC₅₀s against the variants over the IC₅₀ of each PI against wild-type HIV_{104pre}. HIV_{11MIX}^{P5} was more resistant to each of the 5 PIs, while DRV and TPV remained fairly active against both

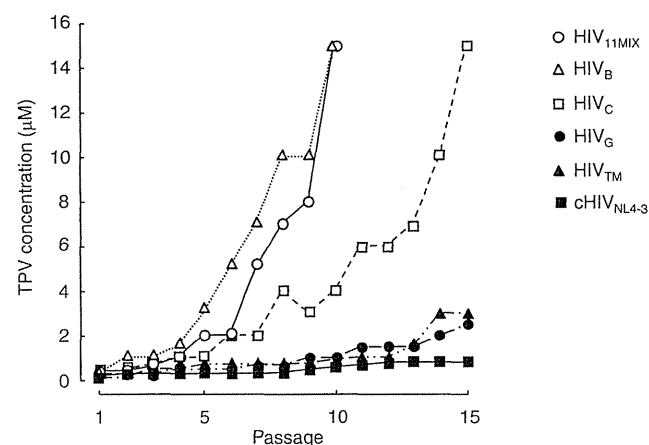


FIG 2 *In vitro* selection of TPV-resistant variants using multidrug-resistant clinical HIV-1 isolates. A mixture of 11 multi-PI-resistant HIV-1 isolates (HIV_{11MIX}), four multidrug-resistant clinical HIV-1 isolates (HIV_B, HIV_C, HIV_G, and HIV_{TM}), and an infectious molecular HIV-1 clone (cHIV_{NL4-3}) were propagated in the presence of increasing concentrations of TPV in MT-4 cells. The selection was carried out in a cell-free manner for a total of 10 to 15 passages with drug concentrations escalating from the IC₅₀ for each virus up to 15 μM. The nucleotide sequences of proviral DNA were determined using the cell lysates of HIV-1-infected MT-4 cells at the termination of each indicated passage.

HIV_{11MIX}^{P0} and HIV_{11MIX}^{P5}, with fold changes of 1 to 8 (Table 2). HIV_{11MIX}^{P10} showed high levels of resistance to the 5 PIs (IC₅₀s for all drugs, >1 μM). HIV_{11MIX}^{P10} was resistant to TPV with a fold change of >34, while it remained relatively susceptible to DRV with a fold change of 10. Of note, the absolute IC₅₀ of DRV against HIV_{11MIX}^{P10} was 0.034 ± 0.004 μM, while that of TPV was >10 μM (Table 2), indicating that the TPV-selected HIV-1 variant was yet fairly susceptible to DRV.

I54V and V82T are major substitutions associated with HIV_{11MIX} acquisition of TPV resistance. We determined the amino acid sequences of the protease in HIV-1 clones prepared at various selection passages of each viral population. In HIV_{11MIX}^{P0}, the original protease sequences of the four isolates HIV_B, HIV_C, HIV_G, and HIV_{TM} (see Fig. S1 in the supplemental material for each sequence) were predominantly identified (3 of 20 clones, 9 of 20 clones, 6 of 20 clones, and 2 of 20 clones, respectively), while the original sequence of HIV_B protease appeared to be the most predominant in HIV_{11MIX}^{P5} and HIV_{11MIX}^{P10}, as shown in Fig. 3A. Of note, I54V was present in the protease of 12 of 20 HIV_{11MIX}^{P0} clones, while it was present in all clones generated from HIV_{11MIX}^{P5} and HIV_{11MIX}^{P10}. V82A was present in all clones of HIV_{11MIX}^{P0} and HIV_{11MIX}^{P5} (20 of 20 clones), while it had been converted to V82T in all clones of HIV_{11MIX}^{P10} (20 of 20 clones) (Fig. 3A), in line with the results previously reported by Baxter et al. (4).

We also analyzed the amino acid sequences of the protease of the four TPV-selected primary HIV-1 strains. I54V was present in 4 of 20 clones of HIV_B^{P0}, while it was found in all clones of HIV_B^{P10}. Similarly, I54V was seen in 16 of 20 clones and 18 of 20 clones of HIV_C^{P0} and HIV_{TM}^{P0}, respectively, while it was seen in all clones of HIV_C^{P15} and HIV_{TM}^{P15}. As seen in the case of HIV_{11MIX}, V82A was seen in 20, 16, 20, and 18 of 20 clones of HIV_B^{P0}, HIV_C^{P0}, HIV_G^{P0}, and HIV_{TM}^{P0}, respectively, and V82T was seen in all clones of HIV_B^{P10}, HIV_C^{P15}, HIV_G^{P15}, and HIV_{TM}^{P15}, as illustrated in Fig. 3B. The results that I54V and V82T were seen in all clones by passage 10 in HIV_{11MIX} and 3 of the 4 primary HIV-1 strains at passage 10 and/or passage 15 suggested that these two amino acid substitutions may represent major amino acid substitutions presumably responsible

TABLE 2 Sensitivities of TPV-resistant variants to various PIs^a

Virus	IC ₅₀ , mean ± SD (μM) (fold change)						
	SQV	IDV	APV	LPV	ATV	DRV	TPV
HIV _{104pre}	0.0043 ± 0.0004	0.033 ± 0.002	0.031 ± 0.001	0.031 ± 0.001	0.0036 ± 0.0001	0.0035 ± 0.0002	0.29 ± 0.03
HIV _{11MIX} ^{P0}	0.036 ± 0.002 (8)	0.97 ± 0.007 (29)	0.31 ± 0.003 (10)	0.34 ± 0.04 (11)	0.043 ± 0.005 (12)	0.015 ± 0.001 (4)	0.32 ± 0.01 (1)
HIV _{11MIX} ^{P5}	0.21 ± 0.08 (48)	>1 (>30)	0.32 ± 0.01 (10)	>1 (>32)	0.38 ± 0.04 (105)	0.021 ± 0.008 (6)	2.5 ± 0.01 (8)
HIV _{11MIX} ^{P10}	>1 (>233)	>1 (>30)	>1 (>32)	>1 (>32)	>1 (>280)	0.034 ± 0.004 (10)	>10 (>34)

^a IC₅₀s were determined by employing MT-4 cells exposed to each virus (50 TCID₅₀s) in the presence of each PI, and the inhibition of p24 Gag protein production was used as the endpoint. All values were determined in triplicate, and the data are shown as mean values ± 1 standard deviation of the results from two or three independent experiments. The numbers in parentheses are changes (*n*-fold) in the IC₅₀ for each isolate compared to the IC₅₀ of each PI for HIV_{104pre}.

for the initiation and/or progression of the development of TPV resistance.

I54V and V82T substitutions do not significantly compromise TPV activity to block protease dimerization. We previously reported that TPV inhibits the dimerization of wild-type HIV-1 protease, as examined with the FRET-based HIV-1 expression system (21). Figure 4A demonstrates the dimerization inhibition profiles of TPV and DRV against wild-type HIV-1 protease. In this assay, COS7 cells were exposed to various concentrations of TPV, DRV, or APV and subsequently transfected with pHIV-PR_{WT}^{CFP} and pHIV-PR_{WT}^{YFP}, and the CFP^{A/B} ratios were determined at the end of the 72-h period of culture. In the absence of drug, the average CFP^{A/B} ratio was 1.06, indicating that protease dimerization occurred in the absence of TPV in the system. In the presence of 0.1 μM TPV, the average CFP^{A/B} ratio was 1.10, indicating that the dimerization still occurred. However, in the presence of 1 and 10 μM TPV, the average CFP^{A/B} ratios were 0.85 and 0.64, respectively, indicating that TPV at both concentrations clearly blocked the dimerization of HIV-1 protease. In contrast, DRV was active in blocking the dimerization at 0.1 μM, with the average ratio being 0.72, while APV failed to block the dimerization at 1 μM (Fig. 4A), as previously reported (21).

We next asked whether amino acid substitutions identified under the selection with TPV affected the dimerization inhibition activity by TPV. As shown in Fig. 3A and B, I54V was seen in all HIV_{11MIX} clones by passage 5 and beyond in all clones of HIV_{11MIX}^{P10}, HIV_B^{P10}, HIV_C^{P15}, and HIV_{TM}^{P15}. It was noted that all the clones of passage 0 virus populations (HIV_B^{P0}, HIV_C^{P0}, HIV_G^{P0}, and HIV_{TM}^{P0}) contained V82A or V82I; however, by passage 10 or 15, all clones contained V82T, strongly suggesting that another base change produced V82A (bases for V and A were GTC and GCC, respectively) and V82I (bases for I were ATC), resulting in acquisition of V82T (bases for T were ACC) (Fig. 3B).

We therefore examined the effects of the I54V and V82T substitutions on the susceptibility of cloned HIV_{NL4-3}^{I54V} (cHIV_{NL4-3}^{I54V}), cHIV_{NL4-3}^{V82T}, and cHIV_{NL4-3}^{I54V/V82T} to the dimerization inhibition activity of TPV. As shown in Fig. 4B, in the presence of 1 and 10 μM TPV, the respective CFP^{A/B} ratios for cHIV_{NL4-3}^{I54V} were 0.91 and 0.88, those for cHIV_{NL4-3}^{V82T} were 0.92 and 0.88, and those for cHIV_{NL4-3}^{I54V/V82T} were 0.86 and 0.81 (Fig. 4B), signifying that I54V and V82T do not significantly affect the dimerization process of protease with the genetic background of cHIV_{NL4-3}.

We also examined the effects of the I54V and V82T substitutions on the susceptibility of protease with the genetic background of HIV_B to TPV's dimerization inhibition activity by generating and testing pHIV-PR_{WT}^{CFP}- and pHIV-PR_{WT}^{YFP}-tagged cHIV_B^{I54V} and cHIV_B^{I54V/V82T} in the FRET-based HIV-1 expres-

sion assay (Fig. 4B). In the absence of TPV, the CFP^{A/B} ratio for cHIV_B was 1.02, and the ratios in the presence of 1 and 10 μM TPV were 1.15 and 0.94, respectively. The ratios seen with cHIV_B^{I54V} and cHIV_B^{I54V/V82T} in the absence of TPV were both 1.12, signifying that the presence of the I54V and V82T substitutions *per se* does not compromise the dimerization process of protease with the genetic background of HIV_B. In the presence of 1 and 10 μM TPV, the CFP^{A/B} ratios for cHIV_B^{I54V} were 1.29 and 0.98, respectively (Fig. 4B). These data suggested that 1 μM TPV failed to block the dimerization of cHIV_B^{I54V} protease, while 10 μM TPV barely blocked the dimerization. The ratios with cHIV_B^{I54V/V82T} in the presence of 1 and 10 μM TPV were 1.19 and 1.0, respectively, indicating that 10 μM TPV did not significantly block the dimerization of cHIV_B^{I54V/V82T} protease. However, DRV at 0.1 μM effectively blocked the dimerization of cHIV_B^{I54V/V82T} protease, suggesting that DRV is more potent in blocking protease dimerization than TPV and/or that the way in which DRV blocks the dimerization of protease monomers differs from that of TPV.

L24M, L33I, and L33F are associated with the loss of TPV's dimerization inhibition. HIV_C originally contained the L24I substitution in its protease (see Fig. S1 in the supplemental material), and this substitution converted to L24M in HIV_C^{P15} in the presence of the selection pressure with TPV (Fig. 3B). In order to examine the impact of L24M on the susceptibility of HIV_C to TPV's dimerization inhibition activity, we introduced L24I and L24M into the protease in the FRET-based HIV-1 expression assay, and the clones were designated cHIV_{NL4-3}^{L24I} and cHIV_{NL4-3}^{L24M}, respectively. TPV at 1 and 10 μM effectively inhibited the dimerization of the protease of cHIV_{NL4-3}^{L24I}, giving average ratios of 0.85 and 0.79, respectively (Fig. 4C). In contrast, upon the introduction of L24M (cHIV_{NL4-3}^{L24M}), both 1 and 10 μM TPV failed to block the dimerization, giving ratios of 1.32 and 1.26, respectively.

L33I was also identified in all HIV_{11MIX}^{P5} and HIV_{11MIX}^{P10} clones examined, although 3 of 20 HIV_{11MIX}^{P0} clones had L33I. Reportedly, the L33F substitution in protease is frequently seen in HIV-1 isolates from patients failing TPV-containing regimens (24, 28). Thus, we introduced L33I and L33F into the protease in the FRET-based HIV-1 expression assay, and the clones were designated cHIV_{NL4-3}^{L33I} and cHIV_{NL4-3}^{L33F}, respectively. TPV at both 1 and 10 μM failed to block the dimerization of the protease of cHIV_{NL4-3}^{L33I}, giving average ratios of 1.11 and 1.03, respectively (Fig. 4C). TPV also failed to block the dimerization of the cHIV_{NL4-3}^{L33F} protease at both 1 and 10 μM.

Moreover, to confirm the responsibility of L33I for compromising TPV's dimerization inhibition, we reverted L33I to the wild-type amino acid (Leu-33) in cHIV_B, cHIV_B^{I54V}, and

A		10	20	30	40	50	60	70	80	90	99	apparently originated from				
cHIV _{NL4-3}		PQITLWQRPL	VTIKIGGQLK	EALLDTGADD	TVLEEMNLPG	RWKPKMIGGI	GGFIKVRQYD	QILIEICGHK	AIGTVLVGPT	PVNIIGRNLL	TQIGCTLNF					
HIV _{11MIX} ^{P6}		I	V	R	I	I	L	V	VP	Q	A	M	8/20	HIV _C		
		I	IE	V	I	I	K	L	P	T	A	M	4/20	HIV _C		
		I	I	I	I	I	I	L	R	VP	V	S	2/20	HIV _B		
		I	R	I	I	I	K	L	R	V	P	V	2/20	HIV _{TM}		
		I	IE	V	I	I	K	L	R	P	T	A	1/20	HIV _C		
		I	IE	V	I	I	K	R	L	P	T	A	1/20	HIV _C		
		I	V	R	I	I	K	L	R	VP	Q	A	1/20	HIV _C		
		I	I	I	I	I	I	L	R	VP	V	S	1/20	HIV _B		
HIV _{11MIX} ^{P5}		I	I	I	I	I	I	V	R	VP	V	S	13/20	HIV _B		
		I	I	P	I	I	I	V	R	VP	V	S	1/20	HIV _B		
		I	I	I	E	I	I	V	R	VP	V	S	1/20	HIV _B		
		I	I	I	I	R	I	V	R	VP	V	S	1/20	HIV _B		
		I	I	I	I	I	V	V	R	VP	V	S	1/20	HIV _B		
		I	I	I	I	I	I	V	R	VPM	V	S	1/20	HIV _B		
		I	I	I	I	I	I	V	R	VP	V	S	1/20	HIV _B		
		I	I	I	I	I	I	V	R	VP	V	S	1/20	HIV _B		
HIV _{11MIX} ^{P10}		I	I	I	I	I	I	V	R	VP	V	S	16/20	HIV _B		
		T	I	I	I	I	I	V	R	VP	V	S	1/20	HIV _B		
		I	I	I	I	R	I	V	R	VP	V	S	1/20	HIV _B		
		I	I	I	I	I	V	V	R	VP	V	S	1/20	HIV _B		
		I	I	I	I	I	I	S	V	R	VP	V	1/20	HIV _B		
B		10	20	30	40	50	60	70	80	90	99					
cHIV _{NL4-3}		PQITLWQRPL	VTIKIGGQLK	EALLDTGADD	TVLEEMNLPG	RWKPKMIGGI	GGFIKVRQYD	QILIEICGHK	AIGTVLVGPT	PVNIIGRNLL	TQIGCTLNF					
HIV _B ^{P0}		I	I	I	I	I	L	R	VP	V	S	A	M	14/20		
		I	I	I	I	I	I	V	R	VP	V	S	A	M	4/20	
		T	I	I	I	I	I	L	R	VP	V	S	A	M	1/20	
		I	I	I	I	I	E	L	R	VP	V	S	A	M	1/20	
HIV _B ^{P10}		I	I	I	DI	I	I	V	R	VP	V	S	T	M	18/20	
		I	I	E	I	DI	I	I	V	R	VP	V	S	T	M	1/20
		I	I	I	DI	I	I	V	R	VP	V	S	A	T	M	1/20
HIV _C ^{P0}		I	V	R	I	I	L	V	VP	Q	A	M		13/20		
		P	V	R	I	I	L	V	VP	Q	A	M		1/20		
		I	T	V	R	I	L	E	V	VP	Q	A	M	1/20		
		I	V	R	I	I	L	V	VPV	Q	A	M		1/20		
		I	V	R	I	I	L	M	VP	Q	I	V	M	2/20		
		I	VW	R	I	I	L	M	VP	Q	I	V	M	1/20		
		I	V	R	I	I	L	M	R	VP	Q	I	V	M	1/20	
HIV _C ^{P15}		I	V	R	M	DI	L	V	VP	Q	T	V	M	10/20		
		I	V	R	M	GI	L	V	VP	Q	T	V	M	6/20		
		I	V	R	M	DI	L	VE	VP	Q	T	V	M	1/20		
		I	V	R	M	DI	EL	V	VP	Q	T	V	M	1/20		
		I	V	R	M	DI	L	V	VP	R	Q	T	V	M	1/20	
		I	V	R	M	DI	L	V	VP	Q	T	V	DM	1/20		
HIV _C ^{P0}		I	IE	V	I	K	L	P	T	A	M		14/20			
		I	IE	V	I	K	L	P	R	T	A	M		2/20		
		A	IE	V	I	K	L	P	T	A	M		1/20			
		I	IE	V	I	K	L	P	T	A	M		1/20			
		I	IE	V	I	W	K	L	P	T	A	M		1/20		
		I	IE	V	I	K	L	PL	T	A	M		1/20			
HIV _C ^{P15}		I	IE	V	I	K	RL	P	T	T	M		16/20			
		P	IE	V	I	K	RL	P	T	T	M	R	1/20			
		I	IE	A	I	K	RL	P	T	T	M		1/20			
		I	IE	V	I	G	RL	P	T	T	M		1/20			
		I	IE	V	I	G	RL	P	T	T	QM		1/20			
HIV _{TM} ^{P0}		I	R	K	L	V	R	P	V	A	V	M	L	8/20		
		I	R	K	L	V	R	P	V	A	V	M	L	6/20		
		I	R	K	L	M	P	Q	I	V	M	L	2/20			
		R	I	R	K	L	V	P	V	A	V	M	L	1/20		
		I	R	K	L	V	R	P	V	A	V	M	L	1/20		
		I	R	K	LM	V	R	P	V	A	V	M	L	1/20		
HIV _{TM} ^{P15}		I	R	K	L	V	R	P	V	T	M	L	L	11/20		
		I	R	K	L	V	R	P	V	T	M	L	L	6/20		
		A	I	R	K	L	V	P	V	T	M	L	L	1/20		
		I	A	R	K	L	V	P	V	T	M	L	L	1/20		
		I	R	K	L	R	V	P	V	T	M	L	L	1/20		

FIG 3 Amino acid sequences of protease-encoding regions of HIV_{11MIX}, HIV_B, HIV_C, HIV_G, and HIV_{TM} on TPV selection. Shown are the amino acid sequences deduced from the nucleotide sequences of the protease-encoding region of proviral DNA isolated from HIV_{11MIX} at passages 1, 5, and 10 (A) and HIV_B, HIV_C, HIV_G, and HIV_{TM} at passages 1 and 10 or 15 (B) in the TPV selection. The consensus sequence of cHIV_{NL4-3} is illustrated at the top as a reference. Identity with the consensus sequence at individual amino acid positions is indicated by dots. The fractions of the virus from which each clone is presumed to have originated over the number of clones examined are shown on the right.

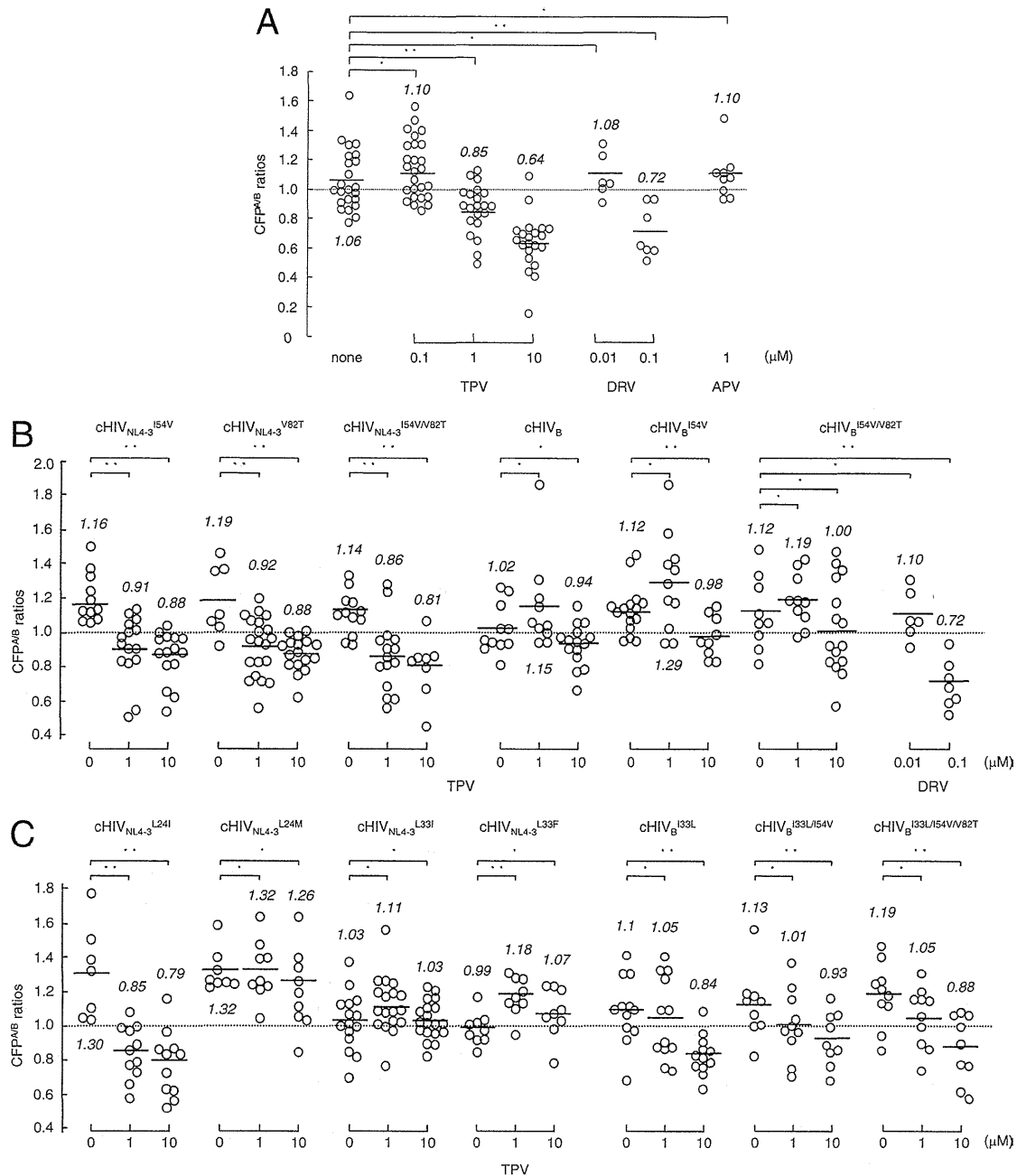


FIG 4 Impact of amino acid substitutions on TPV's dimerization inhibition. (A) COS7 cells were exposed to each of the drugs (TPV, DRV, and APV) at various concentrations and subsequently cotransfected with plasmids encoding each full-length molecular infectious HIV-1 (HIV_{NL4-3}) clone producing CFP- or YFP-tagged wild-type protease. After 72 h, cultured cells were examined in the FRET-HIV-1 assay system and the CFP^{A/B} ratios were determined. The mean values of the ratios obtained are shown as bars. A CFP^{A/B} ratio that is greater than 1 signifies that protease dimerization occurred, whereas a ratio that is less than 1 signifies the disruption of protease dimerization. All the experiments were conducted in a blind fashion. *, not significant; **, $P < 0.05$. (B) COS7 cells were cotransfected with a pair of clones, pHIV_{NL4-3}^{CFP} and pHIV_{NL4-3}^{YFP}, carrying I54V (cHIV_{NL4-3}^{I54V}), V82T (cHIV_{NL4-3}^{V82T}), or I54V/V82T (cHIV_{NL4-3}^{I54V/V82T}) or a pair of clones, pHIV_B^{CFP} and pHIV_B^{YFP}, carrying no additional substitution (cHIV_B), I54V (cHIV_B^{I54V}), or I54V/V82T (cHIV_B^{I54V/V82T}) in the absence or presence of 1 or 10 μM TPV or 0.01 or 0.1 μM DRV, and CFP^{A/B} ratios were determined. *, not significant; **, $P < 0.05$. The statistical differences (P values) between the CFP^{A/B} ratios in the absence of drug (CFP^{A/B}_{no drug}) and the CFP^{A/B} ratios in the presence of 1 μM TPV (CFP^{A/B}_{1 TPV}) and those between the CFP^{A/B} ratios in the absence of drug (CFP^{A/B}_{no drug}) and the CFP^{A/B} ratios in the presence of 10 μM TPV (CFP^{A/B}_{10 TPV}) were, respectively, < 0.0001 and < 0.0001 for cHIV_{NL4-3}^{I54V}, 0.0067 and 0.0005 for cHIV_{NL4-3}^{V82T}, 0.0009 and 0.0005 for cHIV_{NL4-3}^{I54V/V82T}, 0.359 and 0.2865 for cHIV_B, 0.132 and 0.0234 for cHIV_B^{I54V}, and 0.3689 and 0.1653 for cHIV_B^{I54V/V82T}. The statistical differences (P values) between the CFP^{A/B} ratios in the absence of drug (CFP^{A/B}_{no drug}) and the CFP^{A/B} ratios in the presence of 0.01 μM DRV (CFP^{A/B}_{0.01 DRV}) and those between the CFP^{A/B} ratios in the absence of drug (CFP^{A/B}_{no drug}) and the CFP^{A/B} ratios in the presence of 0.1 μM DRV (CFP^{A/B}_{0.1 DRV}) were 0.5956 and 0.0021, respectively, for cHIV_B^{I54V/V82T}. (C) COS7 cells were cotransfected with a pair of clones, pHIV_{NL4-3}^{CFP} and pHIV_{NL4-3}^{YFP}, carrying L241, L24M, L33I, or L33F or a pair of clones, pHIV_B^{CFP} and pHIV_B^{YFP}, with Leu-33 (wild-type) reverted from Ile-33 (cHIV_B^{I33L}) with an additional I54V substitution (cHIV_B^{I33L/I54V}) or with an additional I54V/V82T substitution (cHIV_B^{I33L/I54V/V82T}) in the absence or presence of 1 or 10 μM TPV, and CFP^{A/B} ratios were determined. *, not significant; **, $P < 0.05$.

TABLE 3 Effects of L33I, L33F, I54V, and V82T substitutions on the susceptibility of cHIV_{NL4-3} and cHIV_B to TPV^a

Infectious clone	Amino acid substitution(s) in PR	Mean \pm SD IC ₅₀ (μ M)	Fold resistance
cHIV _{NL4-3}	Wild type	0.27 \pm 0.003	1
cHIV _{NL4-3} ^{L33I}	L33I	Does not replicate	
cHIV _{NL4-3} ^{L33F}	L33F	0.27 \pm 0.001	1
cHIV _{NL4-3} ^{I54V}	I54V	0.37 \pm 0.005	1
cHIV _{NL4-3} ^{V82T}	V82T	0.31 \pm 0.025	1
cHIV _{NL4-3} ^{V82L}	V82L	0.33 \pm 0.023	1
cHIV _{NL4-3} ^{L33I/M36I}	L33I, M36I	0.33 \pm 0.004	1
cHIV _{NL4-3} ^{I54V/V82T}	I54V, V82T	0.28 \pm 0.004	1
cHIV _B	L10I, L33I, M36I, M46I, F53L, K55R, I62V, L63P, A71V, G73S, V82A, L90M, I93L	0.30 \pm 0.02	1
cHIV _B ^{I33L}	L10I, M36I, M46I, F53L, K55R, I62V, L63P, A71V, G73S, V82A, L90M, I93L	0.26 \pm 0.03	1
cHIV _B ^{I54V}	L10I, L33I, M36I, M46I, I54V, K55R, I62V, L63P, A71V, G73S, V82A, L90M, I93L	2.9 \pm 0.11	11
cHIV _B ^{I54V/V82T}	L10I, L33I, M36I, M46I, I54V, K55R, I62V, L63P, A71V, G73S, V82T, L90M, I93L	3.2 \pm 0.1	12
cHIV _B ^{I33L/I54V}	L10I, M36I, M46I, I54V, K55R, I62V, L63P, A71V, G73S, V82A, L90M, I93L	1.2 \pm 0.19	4
cHIV _B ^{I33L/I54V/V82T}	L10I, M36I, M46I, I54V, K55R, I62V, L63P, A71V, G73S, V82T, L90M, I93L	2.5 \pm 0.26	9

^a Data shown represent mean values \pm 1 standard deviation derived from the results of three independent experiments conducted in triplicate. The IC₅₀s were determined by employing MT-4 cells exposed to each infectious HIV-1 clone (50 TCID₅₀s) in the presence of each PI and using the inhibition of p24 Gag protein production as the endpoint.

cHIV_B^{I54V/V82T}, generating cHIV_B^{I33L}, cHIV_B^{I33L/I54V}, and cHIV_B^{I33L/I54V/V82T}, respectively, and determined the CFP^{A/B} ratios. TPV failed to inhibit the dimerization of cHIV_B^{I33L}, cHIV_B^{I33L/I54V}, and cHIV_B^{I33L/I54V/V82T} at 1 μ M, while the CFP^{A/B} values were barely over 1.0. In fact, TPV at 10 μ M blocked the dimerization in all three revertants (Fig. 4C). The observed moderately increased susceptibility of the three revertants to TPV's dimerization inhibition appears to confirm that L33I and L33F play a role in compromising TPV's dimerization inhibition activity.

Impact of L33I, L33F, I54V, and V82T substitutions on susceptibility of HIV_{NL4-3} and HIV_B to TPV's antiviral activity. We also examined the impact of the L33I, L33F, I54V, and V82T substitutions on the activity of TPV to block HIV-1 replication. When the L33I substitution was introduced into cHIV_{NL4-3} (designated cHIV_{NL4-3}^{L33I}), cHIV_{NL4-3}^{L33I} failed to replicate, so the IC₅₀ of TPV against cHIV_{NL4-3}^{L33I} could not be determined. However, cHIV_{NL4-3}^{L33I/M36I} propagated fairly well. All of the other 4 newly generated infectious clones, cHIV_{NL4-3}^{L33F}, cHIV_{NL4-3}^{I54V}, cHIV_{NL4-3}^{V82T}, and cHIV_{NL4-3}^{I54V/V82T}, also replicated well, and the IC₅₀s of TPV against these four recombinant clones were readily determined. The IC₅₀s obtained were virtually identical to each other, with fold differences being \sim 1 in comparison with the IC₅₀ of TPV against cHIV_{NL4-3} (Table 3).

When HIV_B was propagated in the presence of increasing concentrations of TPV, all the clones (20/20) derived from the virus at passage 10 (HIV_B^{P10}) had I54V and V82T substitutions, both of which were also seen in all clones (20/20) derived from HIV_C^{P15} and HIV_{TM}^{P15} (Fig. 3B). It is of note that HIV_B^{P10} and HIV_C^{P15} were propagating in the presence of \sim 15 μ M TPV, while HIV_{TM}^{P15} was barely propagating in the presence of 3 μ M TPV. We therefore examined the impact of both I54V and V82T substitutions on the susceptibility of HIV_B to TPV by introducing I54V alone and I54V/V82T into HIV_B, generating cHIV_B^{I54V} and cHIV_B^{I54V/V82T}, respectively. cHIV_B^{I54V} and cHIV_B^{I54V/V82T} were significantly resistant to TPV, with IC₅₀s of 2.9 and 3.2 μ M, respectively, which were 11- and 12-fold increases in comparison to the IC₅₀ against cHIV_B, respectively (Table 3). Prior to the TPV selection, HIV_B had contained the L33I substitution (see Fig. S1 in the supplemental material) and the HIV_{11MIX}^{P0} population had

the L33I substitution in 3 of 20 clones; however, L33I became predominant by passage 5 (20 of 20 clones; Fig. 3A). Thus, as mentioned above, we reverted L33I to the wild-type amino acid (Leu-33) in cHIV_B, cHIV_B^{I54V}, and cHIV_B^{I54V/V82T}, generating cHIV_B^{I33L}, cHIV_B^{I33L/I54V}, and cHIV_B^{I33L/I54V/V82T}, respectively, and determined their susceptibility to TPV. The susceptibility of cHIV_B^{I33L} to TPV was similar to that of cHIV_{NL4-3}; however, both cHIV_B^{I33L/I54V} and cHIV_B^{I33L/I54V/V82T} were less resistant to TPV (with fold differences in IC₅₀s of 4 and 9, respectively) than their counterparts, cHIV_B^{I54V} and cHIV_B^{I54V/V82T}, respectively (which had fold differences of 11 and 12, respectively) (Table 3). These data suggest that (i) the L33I substitution alone is detrimental to the viral fitness of cHIV_{NL4-3}, (ii) the L33I substitution renders cHIV_{NL4-3} resistant to TPV inhibition of protease dimerization, (iii) the L33I substitution alone does not significantly change the antiviral susceptibility of cHIV_B to TPV, and (iv) with the genetic background of cHIV_B, L33I in the presence of I54V and I54V/V82T contributes to the acquisition of relatively greater resistance to TPV, probably through compromising TPV's dimerization inhibition activity.

Impact of L24I, L24M, E35D, V82T, and I84V substitutions on the susceptibility of HIV_{NL4-3} and HIV_B to TPV's antiviral activity. Upon the selection of HIV_C with TPV, by passage 15, L24I had been converted to L24M (20 of 20 clones) and E35D (15 of 20 clones), V82T (20 of 20), and I84V (20 of 20) had newly emerged (Fig. 3B). Thus, we assessed the effects of such amino acid substitutions on the susceptibility of HIV_C to TPV's antiviral activity. Interestingly, the introduction of L24I and L24M substitutions rendered cHIV_{NL4-3} (cHIV_{NL4-3}^{L24I} and cHIV_{NL4-3}^{L24M}, respectively) more susceptible to TPV, with IC₅₀s of 0.02 and 0.029 μ M, respectively, compared with an IC₅₀ of 0.27 μ M against cHIV_{NL4-3} (Table 4). However, when L24I and L24M were present with the genetic background of HIV_C, the IC₅₀s of TPV were 0.24 μ M (0.9-fold difference) and 0.6 μ M (2.2-fold difference), respectively, suggesting that L24M is associated with the moderate resistance of HIV_C to TPV. The introduction of V82T into HIV_C made the virus slightly resistant to TPV, with an IC₅₀ of 0.38 μ M (1.4-fold difference). However, HIV_C with the combination of three amino acid substitutions, cHIV_C^{L24M/E35D/V82T}, was significantly more resistant to TPV. HIV_C with four substitutions,

TABLE 4 Effects of L24I, L24M, E35D, V82T, and I84V substitutions on the susceptibility of cHIV_{NL4-3} and cHIV_C to TPV^a

Infectious clone	Amino acid substitution(s) in PR	Mean \pm SD IC ₅₀ (μ M)	Fold resistance
cHIV _{NL4-3}	Wild type	0.27 \pm 0.003	1
cHIV _{NL4-3} ^{L24I}	L24I	0.02 \pm 0.003	0.07
cHIV _{NL4-3} ^{L24M}	L24M	0.029 \pm 0.003	0.1
cHIV _C	L10I, I15V, K20R, L24I, M36I, M46L, I54V, I62V, L63P, K70Q, V82A, L89M	0.24 \pm 0.06	0.9
cHIV _C ^{L24M}	L10I, I15V, K20R, L24M, M36I, M46L, I54V, I62V, L63P, K70Q, V82A, L89M	0.6 \pm 0.02	2.2
cHIV _C ^{V82T}	L10I, I15V, K20R, L24I, M36I, M46L, I54V, I62V, L63P, K70Q, V82T, L89M	0.38 \pm 0.01	1.4
cHIV _C ^{L24M/E35D/V82T}	L10I, I15V, K20R, L24M, E35D, M36I, M46L, I54V, I62V, L63P, K70Q, V82T, L89M	1.95 \pm 0.04	7.2
cHIV _C ^{L24M/E35D/V82T/I84V}	L10I, I15V, K20R, L24M, E35D, M36I, M46L, I54V, I62V, L63P, K70Q, V82T, I84V, L89M	2.25 \pm 0.13	8.3

^a Antiviral data shown represent mean values \pm 1 standard deviation derived from the results of three independent experiments conducted in triplicate. The IC₅₀s were determined by employing MT-4 cells exposed to each infectious HIV-1 clone (50 TCID₅₀s) in the presence of each PI and using the inhibition of p24 Gag protein production as the endpoint.

cHIV_C^{L24M/E35D/V82T/I84V}, was further more resistant to the drug, with an IC₅₀ of 2.25 μ M (8.3-fold difference) (Table 4). These data suggest that all five amino acid substitutions, L24I, L24M, E35D, V82T, and I84V, contribute to the decreased susceptibility of HIV_C, in particular, when combined.

The presence of I54V/V82T expedites HIV_{NL4-3} acquisition of TPV resistance compared to that of L33F. We further examined how the presence of L33F or I54V/V82T affected the acquisition of cHIV_{NL4-3} resistance to TPV by propagating cHIV_{NL4-3}^{L33F} or cHIV_{NL4-3}^{I54V/V82T} in the presence of increasing concentrations of TPV. As shown in Fig. 5, cHIV_{NL4-3}^{I54V/V82T}, followed by cHIV_{NL4-3}^{L33F}, readily started replicating robustly in the presence of up to 5 μ M TPV. cHIV_{NL4-3} was most delayed in its acquisition of replicative ability in the presence of TPV. These data suggest that I54V/V82T substitutions are associated with TPV resistance with the genetic background of cHIV_{NL4-3} and prompt HIV-1's development of TPV resistance, while these two substitutions do not affect the susceptibility of protease to TPV's dimerization inhibition activity with the genetic background of cHIV_{NL4-3} (Fig. 4B).

Determination of the amino acid sequences of cHIV_{NL4-3}^{I54V/V82T}

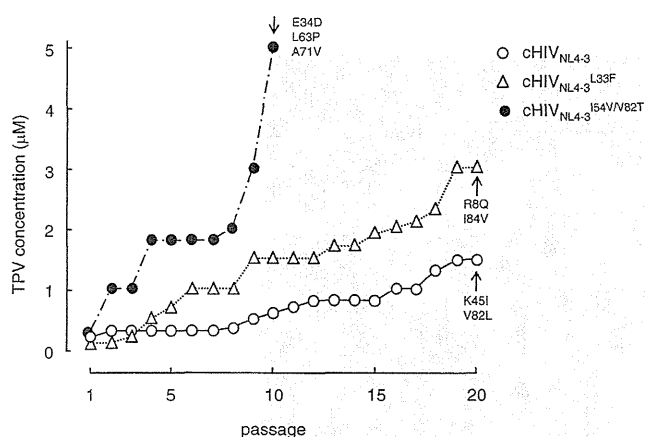


FIG 5 *In vitro* selection of TPV-resistant variants using HIV-1 carrying L33F or I54V/V82T. cHIV_{NL4-3} (○), cHIV_{NL4-3}^{L33F} (△), and cHIV_{NL4-3}^{I54V/V82T} (●) were propagated in the presence of increasing concentrations of TPV (starting at 0.3 μ M) in MT-4 cells. The selection was carried out in a cell-free manner for a total of 10 or 20 passages. Amino acid substitutions identified in the protease of each HIV-1 strain at the conclusion of each passage of the selection are shown with arrows.

at passage 10 revealed that the virus population had additionally acquired E34D, L63P, and A71V, while cHIV_{NL4-3}^{L33F} had additionally acquired R8Q and E35G (Fig. 5).

E34D renders HIV_{NL4-3} protease resistant to TPV's dimerization inhibition, while other substitutions (L63P, A71V, K45I, or V82L) do not. We finally examined whether each of the amino acid substitutions that emerged during the selection of cHIV_{NL4-3} with TPV altered the susceptibility of cHIV_{NL4-3} protease to TPV's dimerization inhibition (Fig. 6). As examined in the FRET-based HIV-1 expression assay, E34D rendered the cHIV_{NL4-3} protease resistant to TPV's dimerization inhibition, while none of the four other substitutions (L63P, A71V, K45I, or V82L) changed the susceptibility of cHIV_{NL4-3} protease to TPV's dimerization inhibition. These data suggest that certain amino acid substitutions that emerge under selection with TPV are associated with the loss of TPV's dimerization inhibition activity, although other substitutions do not affect the susceptibility of protease to TPV's dimerization inhibition activity but contribute to the acquisition of HIV-1's TPV resistance. Hence, there are two distinct types of amino acid substitutions contributing to the acquisition of HIV-1's TPV resistance with the genetic background of cHIV_{NL4-3}: (i) amino acid substitutions conferring the loss of TPV's dimerization inhibition on protease and (ii) those contributing to the acquisition of HIV resistance to TPV without affecting its susceptibility to TPV's dimerization inhibition activity.

DISCUSSION

TPV is a Food and Drug Administration (FDA)-approved, non-peptidic PI (34). Doyon and her colleagues have reported that the development of HIV-1 resistance to TPV is slow and requires 9 months of sequential passage as well as multiple amino acid substitutions in culture (9). Indeed, when cHIV_{NL4-3} was used as a starting HIV-1 strain in the present study, cHIV_{NL4-3} failed to start replicating in the presence of TPV (Fig. 2), which is in line with the data presented by Doyon et al. (9). However, as shown in Fig. 2, three HIV-1 populations (HIV_{11MIX}, HIV_B, and HIV_C) readily started propagating in the presence of increasing concentrations of TPV. This observation confirms that the use of a mixture of multiple-drug-resistant clinical strains and certain highly multi-PI-resistant clinical strains makes it possible to substantially more readily obtain otherwise hard-to-select drug-resistant HIV-1 variants, as previously described (19). Of note, all the clinical strains employed as a source of the mixed HIV-1 population in the pres-